ISSN 1974-4110 (on line edition)
ISSN 1594-7645 (print edition)

Università
degli Studi di Urbino
"Carlo Bo"

Facoltà
di Economia

www.econ.uniurb.it

WP-EMS

Working Papers Series in

Economics, Mathematics and Statistics

"2D discontinuous piecewise linear map: Emergence of fashion cycles"

- Laura Gardini (Department of Economics, Society and Politics, University of Urbino)
- Iryna Sushko (Institute of Mathematics, NASU, and Kyiv School of Economics, Ukraine)
- Kiminori Matsuyama (Department of Economics, Northwestern University, USA)

WP-EMS # 2017/03

2D discontinuous piecewise linear map: Emergence of fashion cycles

Laura Gardini[a], Iryna Sushko[b], Kiminori Matsuyama[c]
[a]Dept of Economics, Society and Politics, University of Urbino, Italy
[b]Institute of Mathematics, NASU, and Kyiv School of Economics, Ukraine
[c]Dept of Economics, Northwestern University, USA

Abstract

We consider a discrete-time version of the continuous-time fashion cycle model introduced in Matsuyama, 1992. Its dynamics are defined by a 2D discontinuous piecewise linear map depending on three parameters. In the parameter space of the map periodicity regions associated with attracting cycles of different periods are organized in the period adding and period incrementing bifurcation structures. The boundaries of all the periodicity regions related to border collision bifurcations are obtained analytically in explicit form. We show the existence of several partially overlapping period incrementing structures, that is a novelty for the considered class of maps. Moreover, we show that if the time-delay in the discrete time formulation of the model shrinks to zero, the number of period incrementing structures tends to infinity and the dynamics of the discrete time fashion cycle model converges to those of continuous-time fashion cycle model.

Keywords: Fashion cycle model, 2D discontinuous piecewise linear map, Border collision bifurcation, Period adding bifurcation structure, Period incrementing bifurcation structure.

Lead Paragraph

The fashion cycle affects many areas of human activity, not only in dress but also in architecture, music, painting, literature, business practice, political doctrines, and scientific ideas. In [12], Matsuyama proposes the continuous-time fashion cycle model, generated by a game played by Conformists, who want to act or look the same with others, and by Nonconformists, who want to act or look different from others. In [12] it is shown that the dynamical system associated with this game is characterized by discontinuous piecewise linear functions, and, depending on parameters, has either stable fixed points or a limit cycle. In the present paper, we reformulate this model into a discrete-time setting to generate a two-dimensional discontinuous piecewise linear map, which is interesting not only due to its applied meaning but also from the mathematical point of view. The bifurcations occurring in this map lead to a new kind of bifurcation structure of the parameter space, which we describe analytically in explicit form. In particular, we show that the map is characterized by (possibly many coexisting) attracting cycles of different periods, whose periodicity regions, with their border collision bifurcation boundaries, are organized in several different families of period incrementing structures. There are also periodicity regions organized in the period adding bifurcation structure related to one-dimensional restrictions of the map, and the results follow from those known from the bifurcation theory of one-dimensional discontinuous maps. We discuss also the connection between the continuous- and discrete-time fashion cycle models. In particular, we show that if the time-delay in the discrete time formulation shrinks to zero then the number of period incrementing structures goes to infinity and the dynamics of the considered map converge to the dynamics of the original continuous-time model. We conjecture that these results can be extended to a wider class of discontinuous maps.

1 Introduction

In this paper, we consider the *two-dimensional (2D) discontinuous piecewise linear map* that describes the dynamics of a discrete-time version of the continuous-time fashion cycle model proposed in [12]. This map is

interesting not only due to its applied context but also from the mathematical point of view, as it belongs to a class of maps for which the bifurcation theory is still not well developed.

As it is well-known, the existence of a border in a *nonsmooth* map, called also *switching manifold*, at which the map changes its definition, may lead to a collision of an invariant set of the map with this border under variation of some parameter, that may cause a drastic change of the dynamics. Such a phenomenon is called *border collision bifurcation*, BCB for short, and many recent research efforts have focused on the classification of possible BCBs in various classes of nonsmooth maps (see, e.g., the books [22], [3] and references therein). For *continuous* nonsmooth maps, for which a generic BCB can be seen as a local bifurcation, many essential results on the classification have been obtained by means of the related normal forms.[1] For *discontinuous* maps, in contrast, a BCB is not a local phenomenon, because it involves a jump of the value of the map when the switching manifold is crossed, and if such a jump is relatively large the result of a BCB depends on the global properties of the map, which poses a significant challenge.

For example, consider a class of *1D piecewise monotone maps* with one discontinuity point arising when a Poincaré section of a Lorenz-type flow is constructed. Among such maps *1D piecewise increasing maps* called *Lorenz maps* have attracted a lot of research attention (see e.g., [8], [10], [6], [20], to cite a few). In particular, it has been shown that if a Lorenz map is *invertible* in the absorbing interval then it can have only *attracting cycles*, associated with *rational* rotation numbers, which are robust (i.e., persistent under parameter perturbations) as well as non robust *Cantor set attractors* representing the closure of quasiperiodic trajectories, associated with *irrational* rotation numbers.[2] In the parameter space of such maps the so-called *period adding bifurcation structure* is observed, formed by the periodicity regions corresponding to the attracting cycles. These regions are ordered according to the Farey summation rule applied to the related rotation numbers.[3] A Poincaré section of a Lorenz-type flow may lead also to a 1D discontinuous map with *one increasing and one decreasing branches*. In the parameter space of such a map the *period incrementing bifurcation structure* can be observed which is formed by the periodicity regions ordered according to the increasing by k periods of the related attracting cycles, and each two adjacent regions are partially overlapping that corresponds to coexisting attracting cycles. We refer to [5] where the period adding and period incrementing structures are associated with codimension-two BCB points in 1D piecewise monotone maps. Note that for a generic *1D piecewise linear map* with one discontinuity point, which is the simplest representative of piecewise monotone maps, the boundaries associated with period adding and period incrementing structures can be obtained analytically in explicit form.[4]

In the 2D piecewise linear map F considered in the present paper there is a period adding structure which is the standard one being related to a 1D reduction of the 2D map, and there are several period incrementing structures associated with 2D dynamics. The overall bifurcation structure of map F is quite interesting and, to our knowledge, it has not been described before. After a brief description of the fashion cycle model by [12] in Sec.2, we describe map F in Sec.3. It consists of four linear maps where each one is a contraction and whose definition regions are separated by two discontinuity lines. The map depends on three parameters; one of them is the coefficient of the contraction of the linear maps, and the other two are the slopes of the discontinuity lines. The variables of map F are coupled only via the discontinuity lines, and this feature allows us to describe the complete bifurcation structure of the parameter space analytically. In particular, we obtain all the boundaries of the periodicity regions associated with period adding and period incrementing structures in explicit form. The period adding structure, discussed in Sec.4 and 5, is associated with parameter values at which map F is reduced to a 1D discontinuous piecewise linear map, so that the results known for such a class of maps can be applied (for completeness the related results are given in Appendix). Novelty for the considered

[1] For a 1D *continuous* map with one border point a complete classification of BCBs can be proposed using a *1D BCB normal form* represented by the well-known *skew tent map* defined by two linear functions ([7], [11], [15], [23], [18]). For 2D continuous nonsmooth maps with one switching manifold many essential results can be obtained with the help of a *2D BCB normal form* defined by two linear maps ([14], [19], [17]).

[2] Chaotic dynamics in the Lorenz map is possible only if it is *noninvertible* in the absorbing interval.

[3] That is, between the regions corresponding to the cycles with rotation numbers m_1/n_1 and m_2/n_2 such that $|m_1n_2 - m_2n_1| = 1$, there exists a region of the cycle with rotation number $(m_1 + m_2)/(n_1 + n_2)$.

[4] For an overview of the bifurcation scenarios in 1D piecewise linear maps with one discontinuity point, we refer to [2]. These scenarios can be seen as building blocks, as they are also observed in 1D maps with more border points and in nonsmooth maps of higher dimension. For example, period adding structure arises in the parameter space of a 1D continuous bimodal map [16], or in a 2D discontinuous triangular map [21]. In a 2D discontinuous piecewise linear map with one discontinuity line considered in [13] both period adding and period incrementing structures are observed being quite similar to those observed in 1D maps.

class of discontinuous maps is related to period incrementing structures. As we show in Sec.6, in the parameter space of map F there are several such structures which are partially overlapping. Moreover, if the coefficient of the contraction of the linear maps tends to 1 (that corresponds also to the time-delay in the discrete time formulation of the model tending to zero) the number of overlapping period incrementing structures goes to infinity. That leads, in particular, to more than two coexisting attracting cycles (in the paper we present an example with four coexisting cycles). Given that each linear component of map F is a contraction, map F can have neither saddle not repelling cycles, and all the basin boundaries of coexisting attractors are formed by proper segments of the discontinuity lines and their preimages. In Sec.7 we compare the dynamics of our map F and the original continuous-time fashion cycle model. We show that if the time-delay in the discrete time formulation shrinks to zero the dynamics of the discrete time fashion cycle model converges to those of continuous-time fashion cycle model. Some concluding remarks are given in Sec.8.

2 The Matsuyama (1992) fashion cycle model

What is the *fashion cycle*? In [12], it is defined as a collective process of taste changes, in which certain forms of social behavior, or "styles", enjoy temporary popularity only to be replaced by others. This pattern of changes sets the fashion cycle apart from the *social custom*. The fashion cycle is also a recurring process, in which many "new" styles are not so much born as rediscovered. Although most conspicuous in the area of dress, many other areas of human activity are subject to the fashion cycles, including architecture, music, painting, literature, business practice, political doctrines, and scientific ideas. So are many stages of our lives, from the names given to babies to the forms of gravestones.

What causes the fashion cycle? And why does it persist? The key idea put forward in [12] is this. In order for such recurrent patterns of the fashion cycle to emerge, two fundamentally irreconcilable desires for human beings–*Conformity* (i.e., the desire to act or look the same as others) and *Nonconformity* (the desire to act or look different from others)–both must operate. Conformity *alone* would lead to an emergence of the social custom, or convention. Nonconformity *alone* would prevent any discernible patterns from emerging. What is necessary for an emergence of the fashion cycle is a delicate balance between Conformity and Nonconformity.

To capture this idea and to study the social environment that leads to fashion cycles as opposed to social customs, [12] considers the society populated by two types of anonymous players, Conformists and Nonconformists, who play the following dynamic game in continuous time, $t \in [0, \infty)$.

- Each player is continuously matched with another player of either type with some probability. The relative frequency of across-type versus within-type matchings is $m > 0$ for a Conformist and $m^* > 0$ for a Nonconformist.[5]
- Each player takes one of the two actions, A and B, and the opportunity to switch actions follows as an independent, identical Poisson process, whose mean arrival rate is $\alpha > 0$.
- When matched, a Conformist gains a *higher* payoff if he sees his matched partner has the same action with his, instead of the different action. A Nonconformist, on the other hand, gains a *lower* payoff if she sees her matched partner takes the same action with her, instead of the different action.

Let $\lambda_t(\lambda_t^*) \in [0,1]$ denote the fraction of Conformists (Nonconformist) with A at time t. Then, a Conformist is more likely to be matched with someone with A than with someone with B if $P_t \equiv (\lambda_t - 1/2) + m(\lambda_t^* - 1/2) > 0$, in which case, the fraction $1-\lambda_t$ of the Conformists who are currently with B switch to A, when the opportunity to switch actions arrives, which follows the Poisson process with the mean arrival rate $\alpha > 0$. Thus, λ_t changes as $\frac{d\lambda_t}{dt} = \alpha(1-\lambda_t)$ if $P_t > 0$. On the other hand, a Nonconformist is more likely to be matched with someone with A than with someone with B if $P_t^* \equiv (\lambda_t^* - 1/2) + m^*(\lambda_t - 1/2) > 0$, in which case, the fraction λ_t^* of the Nonconformists who are currently with A would switch to B, when the opportunity to switch arrives, so that λ_t^* changes as $\frac{d\lambda_t^*}{dt} = -\alpha\lambda_t^*$ if $P_t^* < 0$. Following this line of logic, the dynamics of $(\lambda_t, \lambda_t^*) \in [0,1]^2$ can be described by the following dynamical system denoted Λ:

[5] These relative frequencies of across-type versus within-type matchings for each type are in turn determined by the relative size of the two types and the relative frequency of the matching being of inter-type versus intra-type.

$$\frac{d\lambda_t}{dt} \in \begin{cases} \{\alpha(1-\lambda_t)\} & \text{if } P_t > 0, \\ [-\alpha\lambda_t, \alpha(1-\lambda_t)] & \text{if } P_t = 0, \\ \{-\alpha\lambda_t\} & \text{if } P_t < 0, \end{cases} \quad \text{where } P_t \equiv (\lambda_t - 1/2) + m(\lambda_t^* - 1/2)$$

$$\frac{d\lambda_t^*}{dt} \in \begin{cases} \{-\alpha\lambda_t^*\}, & \text{if } P_t^* > 0, \\ [-\alpha\lambda_t^*, \alpha(1-\lambda_t^*)], & \text{if } P_t^* = 0, \\ \{\alpha(1-\lambda_t^*)\}, & \text{if } P_t^* < 0, \end{cases} \quad \text{where } P_t^* = (\lambda_t^* - 1/2) + m^*(\lambda_t - 1/2) \tag{1}$$

In [12], it is shown that this dynamical system has effectively three kinds of asymptotic behaviors, depending on the two parameters, $m > 0$ and $m^* > 0$.[6] In particular, for $m^* > m > 1$, there exists a limit cycle, along which Nonconformists become fashion leaders, and switch their actions periodically, while Conformists follow with delay. In fact, this limit cycle can occur through two kinds of bifurcation. First, starting from the case of $m > m^* > 1$, where $(\lambda_t, \lambda_t^*) = (1/2, 1/2)$ is the globally attracting fixed point, an increase in the share of Conformists (a decrease in the share of Nonconformists) leads to a loss of the stability of $(\lambda_t, \lambda_t^*) = (1/2, 1/2)$, which creates of the limit cycle, similar to a Hopf bifurcation.[7] Second, starting from the case of $m^* > 1 > m$, where $(\lambda_t, \lambda_t^*) = (1, 0)$ and $(\lambda_t, \lambda_t^*) = (0, 1)$ are two stable fixed points, whose basins of attraction are separated by $P_0 = 0$ (this case can be interpreted as the Conformists setting the social custom, and the Nonconformists revolting against it), a decrease in the share of Conformists (an increase in the share of Nonconformists) leads to a loss of the stability of both $(\lambda_t, \lambda_t^*) = (1, 0)$ and $(\lambda_t, \lambda_t^*) = (0, 1)$, which creates the limit cycle through a nonsmooth analogue of a heteroclinic bifurcation.

In Sec.7 the dynamics of the continuous-time fashion cycle model (1) are described in more detail to be compared with those of the discrete-time model introduced in the next section.

3 Description of the map. Preliminaries

In the present paper, we reformulate the continuous-time fashion cycle model of [12] into a discrete-time setting as follows. Matching now takes place at a regular interval, $\triangle > 0$, and from the current match and the next match, the fraction $\delta = 1 - e^{-\alpha\triangle} > 0$ of the players can switch actions before the next match. Then, the dynamics of a discrete version of the Matsuyama fashion cycle model can be described by a family of 2D discontinuous piecewise linear maps $F : I^2 \to I^2$, $I^2 = [0, 1] \times [0, 1]$, given by $(x_{n+1}, y_{n+1}) = F(x_n, y_n)$:

$$x_{n+1} = \begin{cases} (1-\delta)x_n + \delta & \text{if } P^x(x_n, y_n) > 0 \\ (1-\delta)x_n & \text{if } P^x(x_n, y_n) < 0 \end{cases}$$

$$y_{n+1} = \begin{cases} (1-\delta)y_n & \text{if } P^y(x_n, y_n) > 0 \\ (1-\delta)y_n + \delta & \text{if } P^y(x_n, y_n) < 0 \end{cases}$$

where

$$P^x(x_n, y_n) = (x_n - 1/2) + m_x(y_n - 1/2), \quad P^y(x_n, y_n) = (y_n - 1/2) + m_y(x_n - 1/2) \tag{2}$$

and the parameters satisfy

$$0 < \delta < 1, \ m_x > 0, \ m_y > 0 \tag{3}$$

Note that parameters m_x, m_y and variables x_n, y_n correspond to parameters m, m^* and variables λ_t, λ_t^*, respectively, in the continuous time formulation of the model.

One can immediately notice that the variables are connected only via the discontinuity lines $P^x(x_n, y_n) = 0$ and $P^y(x_n, y_n) = 0$.[8] Moreover, their dynamics are governed by the discontinuous function consisting of two linear branches with equal slopes $1 - \delta \equiv a$, where $0 < a < 1$, so that map F can have neither repelling or

[6] The asymptotic behaviors are independent of $\alpha > 0$. Indeed, one could set $\alpha = 1$ without loss of generality by rescaling time as $t' = \alpha t$.

[7] Note however that the mechanism of this bifurcation is related to the nonsmoothness of the system and not to a pair of complex-conjugate eigenvalues crossing imaginary axis as it occurs in case of a Hopf bifurcation.

[8] Note that map F is not defined at the discontinuity lines. In fact, such a definition does not influences the overall bifurcation structure of the parameter space which is the main subject of our study. What is really important for the bifurcation analysis are *the limit values of the system function on both sides of the borders.*

saddles cycles, nor chaotic dynamics. Nevertheless, the dynamics of F is quite interesting being characterised by coexisting attracting cycles of different periods and complicated bifurcation structures related to these cycles, which we are going to describe.

The discontinuity lines given in (2) subdivide the phase plane of map F into four regions denoted D_i, $i = \overline{1,4}$, associated with corresponding linear maps F_i. Let us rewrite the definition of map F in the following form using its linear components:

$$\begin{array}{l} F_1 : \begin{pmatrix} x \\ y \end{pmatrix} \mapsto \begin{pmatrix} (1-\delta)x \\ (1-\delta)y + \delta \end{pmatrix}, \text{ for } (x,y) \in D_1 \\ F_2 : \begin{pmatrix} x \\ y \end{pmatrix} \mapsto \begin{pmatrix} (1-\delta)x + \delta \\ (1-\delta)y \end{pmatrix}, \text{ for } (x,y) \in D_2 \\ F_3 : \begin{pmatrix} x \\ y \end{pmatrix} \mapsto \begin{pmatrix} (1-\delta)x \\ (1-\delta)y \end{pmatrix}, \quad \text{for } (x,y) \in D_3 \\ F_4 : \begin{pmatrix} x \\ y \end{pmatrix} \mapsto \begin{pmatrix} (1-\delta)x + \delta \\ (1-\delta)y + \delta \end{pmatrix}, \text{ for } (x,y) \in D_4 \end{array} \tag{4}$$

where

$$\begin{aligned} D_1 &= \{(x,y) \in I^2 : P^x(x,y) < 0,\ P^y(x,y) < 0\} \\ D_2 &= \{(x,y) \in I^2 : P^x(x,y) > 0,\ P^y(x,y) > 0\} \\ D_3 &= \{(x,y) \in I^2 : P^x(x,y) < 0,\ P^y(x,y) > 0\} \\ D_4 &= \{(x,y) \in I^2 : P^x(x,y) > 0,\ P^y(x,y) < 0\} \end{aligned}$$

Property 1. Map F is symmetric with respect to (wrt for short) the point $(x,y) = (1/2, 1/2)$ denoted S.

One can check that for points $p = (x,y)$ and $p' = (1-x, 1-y)$ which are symmetric wrt S it holds that $F(p)$ and $F(p')$ are also symmetric wrt S. This property implies

Property 2. Any invariant set A of map F is either symmetric wrt S or there must exist one more invariant set A' which is symmetric to A wrt S.

The discontinuity lines $P^x(x,y) = 0$ and $P^y(x,y) = 0$ can be written as

$$C^x : \quad y = -\frac{1}{m_x}\left(x - \frac{1}{2}\right) + \frac{1}{2}, \qquad C^y : \quad y = -m_y\left(x - \frac{1}{2}\right) + \frac{1}{2} \tag{5}$$

In the (x,y)-plane C^x and C^y are straight lines with negative slopes, intersecting at point S. They coincide if

$$C : \qquad m_y = \frac{1}{m_x} \tag{6}$$

in which case F is defined by the maps F_1 and F_2 only.

Depending on $m_x m_y \gtrless 1$, as well as $m_x \gtrless 1$, $m_y \gtrless 1$, one can distinguish between 6 cases (see Fig.1 and Fig.2) which in short can be characterised as follows:

- For $(m_x, m_y) \in R_I = \{m_x m_y > 1,\ m_x < 1\}$ (**Case I**) and $(m_x, m_y) \in R_{II} = \{m_x m_y < 1,\ m_y > 1\}$ (**Case II**) map F has two attracting border fixed points, $(x,y) = (0,1)$ and $(x,y) = (1,0)$ (the fixed points of F_1 and F_2, respectively). It is easy to see that their basins are separated by the discontinuity line C^x.

- For $(m_x, m_y) \in R_{III} = \{m_y < 1,\ m_x < 1\}$ (**Case III**) map F has either two coexisting attracting n-cycles, $n \geq 2$, denoted γ_n and γ'_n, symmetric to each other wrt S and belonging, respectively, to the left and right border of I^2 (denoted I_0 and I_1), or two coexisting Cantor set attractors, $q_\rho \in I_0$ and $q'_\rho \in I_1$, associated with an irrational rotation number ρ, which are also symmetric to each other wrt S. Similarly to the Cases I and II, the basins of coexisting attractors are separated by C^x. In the (δ, m_x, m_y)-parameter space associated with Case III a *period adding bifurcation structure* is observed which is formed by the periodicity regions related to the border cycles.

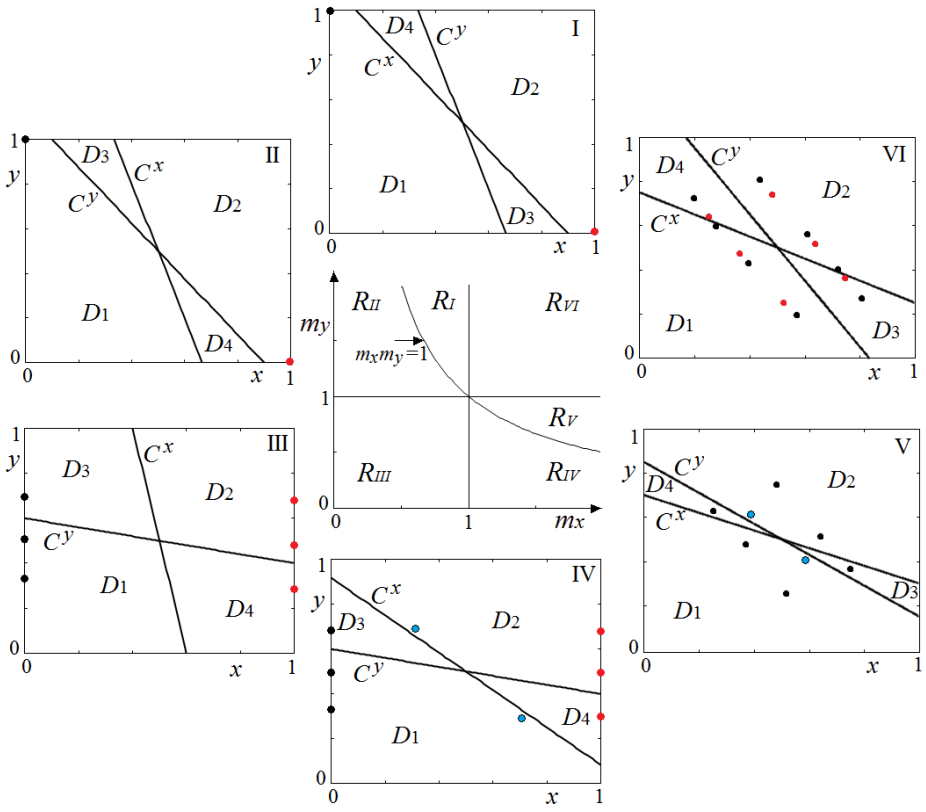

Figure 1: In the center: partitioning of the (m_x, m_y)-parameter plane into the regions R_I, R_{II},..., R_{IV}. Around the center: examples of the discontinuity lines C^x, C^y and attractors of map F associated with these regions.

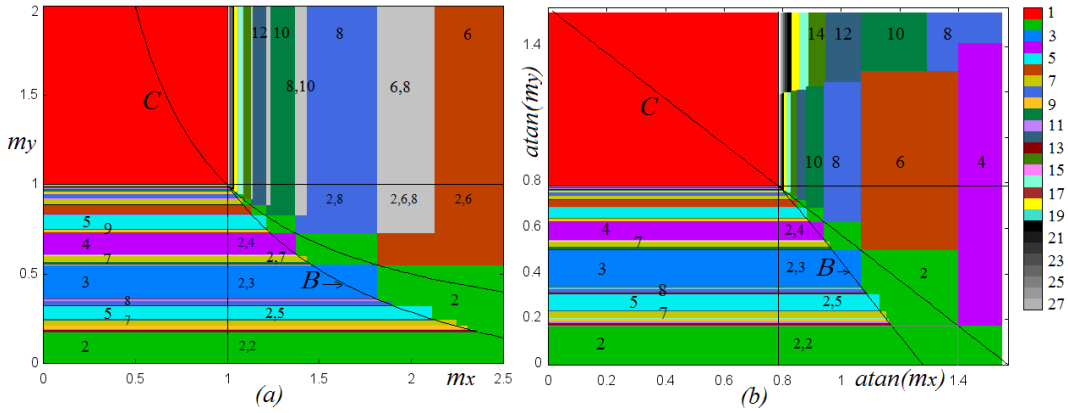

Figure 2: 2D bifurcation diagram of map F in the (m_x, m_y)- and $(\arctan(m_x), \arctan(m_y))$-parameter plane for $\delta = 0.3$. Color panel on the right indicates a correspondence between the colors of the parameter regions and periods of the related cycles (some periods are indicated by numbers). In (a) some coexistence regions are shown in gray.

- For $(m_x, m_y) \in R_{IV} = \{m_x m_y < 1,\, m_x > 1\}$ (**Case IV**) map F has an attracting interior 2-cycle denoted Γ_2 (whose points belong to D_1 and D_2 and are symmetric wrt S), which may coexist or not with border n-cycles $\gamma_n \in I_0$ and $\gamma'_n \in I_1$, or with border Cantor set attractors $q_\rho \in I_0$ and $q'_\rho \in I_1$.

- For $(m_x, m_y) \in R_V = \{m_x m_y > 1,\, m_y < 1\}$ (**Case V**) map F has an interior 2-cycle Γ_2 which may coexist or not with one interior $2n$-cycle Γ_{2n}, $n \geq 2$, or with two interior cycles, Γ_{2n} and $\Gamma_{2(n+1)}$ (each of these cycles is symmetric wrt S). In the parameter space the related periodicity regions are organised in a *period incrementing bifurcation structure* with incrementing step 2.

- For $(m_x, m_y) \in R_{VI} = \{m_x > 1,\, m_y > 1\}$ (**Case VI**) map F has one or several coexisting interior cycles of even periods. In the parameter space there are $\bar{l} \geq 1$ period incrementing bifurcation structures, which are partially overlapping, where $\bar{l} = \lfloor \log_{1-\delta} 0.5 \rfloor + 1$. Here $\lfloor \cdot \rfloor$ is the floor function which for positive numbers gives the integer part of the number.

Cases I and II are straightforward. Cases III, IV, V and VI are considered in detail in the following sections.

4 Case III: two border n-cycles and period adding structure

For $0 < \delta < 1$ and $(m_x, m_y) \in R_{III}$ any initial point (x_0, y_0) with $y_0 < -\frac{1}{m_x}\left(x - \frac{1}{2}\right) + \frac{1}{2}$, i.e., below the discontinuity line C^x (where the maps F_1 and F_3 are defined) converges to I_0, given that $x \to 0$ as the number of iterations tends to infinity for both maps F_1 and F_3. The dynamics of the y variable on I_0 are governed by the 1D piecewise linear map g defined as follows:

$$g : y \to g(y) = \begin{cases} g_L(y) = (1-\delta)y + \delta, & 0 \leq y < c \\ g_R(y) = (1-\delta)y, & c < y \leq 1 \end{cases} \tag{7}$$

where $c = (m_y + 1)/2 > 1/2$ is the discontinuity point of g. An example of map g is shown in Fig.3a where $\delta = 0.3$, $m_y = 0.5$.

The dynamics of such a class of maps, that is, 1D piecewise linear maps with one discontinuity point and increasing contracting branches, are well studied (see, e.g., [9], [8], [1], [5]). Obviously, such maps cannot have repelling cycles or chaotic invariant sets, but they can have *attracting cycles* of any period. Each such a cycle, which appears/disappears due to BCB[9] is associated with a *rational rotation number*. These cycles are robust, that is persistent under parameter perturbations; in the parameter space the regions associated with existence of these cycles, called *periodicity regions*, are organized in the period adding bifurcation structure. *Irrational rotation numbers* are associated with *Cantor set attractors* (representing the closure of quasiperiodic trajectories) which are not robust (see e.g., [8]). For map g the period adding bifurcation structure in the (δ, m_y)-parameter plane is shown in Fig.4. One can see that there are two boundaries of an n-periodicity region associated with cycle γ_n. These boundaries are related to collision of γ_n with the discontinuity point from the left and right sides. The analytical expressions of these boundaries can be written explicitly (see Appendix). Given that map g does not depend on m_x, in the (m_x, m_y)-parameter plane the boundaries of the periodicity regions in R_{III} are represented by horizontal straight lines (see Fig.2).

The dynamics of initial points (x_0, y_0) with $y_0 > -\frac{1}{m_x}\left(x - \frac{1}{2}\right) + \frac{1}{2}$, i.e., above C^x (where maps F_2 and F_4 are defined), are symmetric wrt S to those described above: any initial point converges to I_1, given that $x \to 1$ as the number of iterations tends to infinity for both maps F_2 and F_4. The dynamics of the y variable on I_1 are defined by the 1D map g' which has the same linear branches as map g and discontinuity point $c' = (1 - m_y)/2 = 1 - c < 1/2$. Due to the symmetry, the bifurcation structure of the (δ, m_y)-parameter plane of map g' is the same as for map g, with the only difference related to the symbolic sequences[10] of the coexisting cycles: if map g has a cycle γ_n then map g' has a symmetric cycle γ'_n whose symbolic sequence is obtained

[9] Recall that a *border collision bifurcation* occurs when under parameter variation an invariant set of a piecewise smooth map collides with a border at which the system function changes its definition, leading to a qualitative change in the dynamics ([14], [15]).

[10] The symbolic sequence of an n-cycle $\{x_i\}_0^{n-1}$ of a map f defined on two partitions, associated with symbols L and R, can be defined as $\sigma = \sigma_0\sigma_1...\sigma_{n-1}$, $\sigma_i \in \{L, R\}$, where $\sigma_i = L$ if $x_i \in L$ and $\sigma_i = R$ if $x_i \in R$.

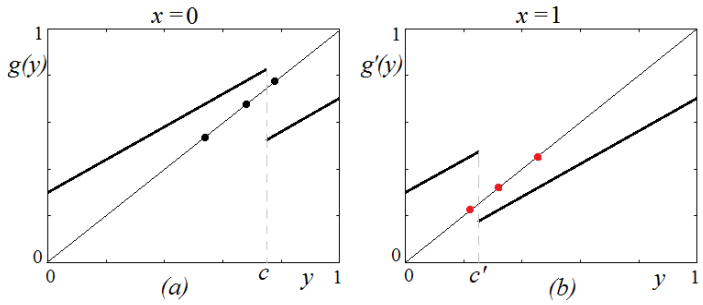

Figure 3: Map g and g' defined on the left and right borders of I^2 are show in (a) and (b), respectively, at $\delta = 0.3$, $m_y = 0.5$ (Case III). Map g has a 3-cycle γ_3 with symbolic sequence L^2R, and map g' has a 3-cycle γ_3' with symbolic sequence R^2L.

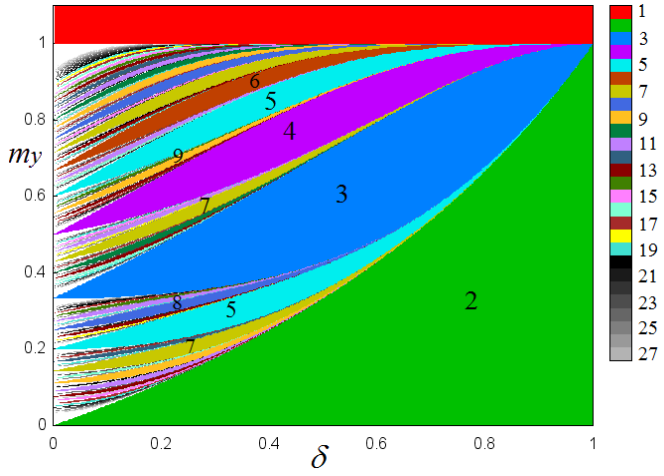

Figure 4: Period adding bifurcation structure in the (δ, m_y)-parameter plane of maps g and g' defined in Case III on the left and right borders of I^2, respectively.

from the symbolic sequence of γ_n interchanging the symbols L and R. For example, if a (δ, m_y)-parameter point belongs to the 3-periodicity region, then both maps, g and g', have attracting 3-cycles, γ_3 with symbolic sequence RL^2 and γ_3' with symbolic sequence LR^2, respectively (see Fig.3).

5 Case IV: interior 2-cycle and two border n-cycles

The transition from Case III to Case IV (for increasing m_x through 1 for some fixed $0 < m_y < 1$) is associated with the appearance of one more discontinuity point on the border I_0 (and on the border I_1) which is the point $(x, y) = (0, d)$ ($(x, y) = (1, 1 - d)$, respectively), where

$$d = \frac{1 + m_x}{2m_x} \tag{8}$$

is the y-coordinate of the intersection point of the discontinuity line C^x with border I_0. After such a transition points of the segment of I_0 (I_1) with $y \in (d, 1)$ ($y \in (0, 1 - d)$), respectively) as well as points of a neighbourhood of this segment, are repelled from the borders. This leads to the appearance of an interior 2-cycle, according to the following

Property 3. For any fixed $0 < \delta < 1$ and $m_x > 1$, $m_y < 1$ map F has an interior attracting 2-cycle $\Gamma_2 = \{p_0, p_1\}$, where

$$p_0 = \left(\frac{1}{2-\delta}, \frac{1-\delta}{2-\delta}\right) \in D_1, \quad p_1 = \left(\frac{1-\delta}{2-\delta}, \frac{1}{2-\delta}\right) \in D_2 \tag{9}$$

To see this, note that considering map $F^2 = F_2 \circ F_1$, its fixed point p_0 is a point of an actual 2-cycle of map F if $p_0 \in D_1$ (in such a case $p_1 = F(p_0) \in D_2$ due to the symmetry), that holds for $m_x > 1$, $m_y < 1$, i.e., for $(m_x, m_y) \in R_{IV} \cup R_V$. For $m_x = 1$ a BCB of Γ_2 occurs at which $p_0 \in C^x$ (and also $p_1 \in C^x$), while for $m_y = 1$ a BCB occurs at which $p_0 \in C^y$ (as well as $p_1 \in C^y$), so that in the (m_x, m_y)-parameter plane the boundaries of the periodicity region associated with an interior 2-cycle are defined by the straight lines $m_y = 1$ and $m_x = 1$.

For $(m_x, m_y) \in R_{IV}$ the 2-cycle $\Gamma_2 = \{p_0, p_1\}$ (see Property 3) may coexist or not with border cycles $\gamma_n \in I_0$ and $\gamma'_n \in I_1$, or, in a non generic case, with Cantor set attractors $q_\rho \in I_0$ and $q'_\rho \in I_1$.

In fact, the periodicity regions forming the period adding structure in region R_{III} extend to region R_{IV}, however, in R_{IV} each region has one more, vertical, boundary (see, for example, Fig.2), related to the mentioned above new discontinuity points $(x, y) = (0, d) \in I_0$ and $(x, y) = (1, 1-d) \in I_1$. To see which bifurcation is associated with this boundary consider map g given in (7) and its absorbing interval $J = [g_R(c), g_L(c)]$ to which the related cycle γ_n belongs (the cycle γ'_n belongs, respectively, to the absorbing interval $J' = [g_R(c'), g_L(c')]$). For $(m_x, m_y) \in R_{IV}$ map g is defined not on the complete border I_0, i.e., not for any $y \in [0, 1]$ as in Case III, but for $y \in [0, d]$, and any point $(x, y) = (0, y)$ with $y > d$ is mapped in the interior of I^2. As long as $g_L(c) < d$, that is, if $d \notin J$, the period adding structure of map F is not influenced by the existence of point d, that is, it extends from region R_{III} to region R_{IV}. If $g_L(c) = d$ that holds for

$$B: \quad m_y = \frac{1 - \delta m_x}{m_x(1-\delta)} \tag{10}$$

the absorbing interval J has a contact with d (see Fig.2 where curve B is shown). If $g_L(c) > d$, i.e., if $d \in J$, new discontinuity point $y = d$ can collide (for increasing m_x) with the rightmost point of cycle γ_n, and this BCB defines the vertical borders of the periodicity regions in R_{IV} (their analytical expressions are given in Appendix). A collision of the discontinuity point $y = c$ can no longer occur with γ_n from the right side (because such a collision means also a collision of the critical point $g_L(c)$ with the rightmost point of γ_n) and, thus, the periodicity regions in R_{IV} have no lower BCB boundary, while such a collision from the left side can still occur (for increasing m_y), and this BCB is associated with the upper boundary of the related periodicity region.

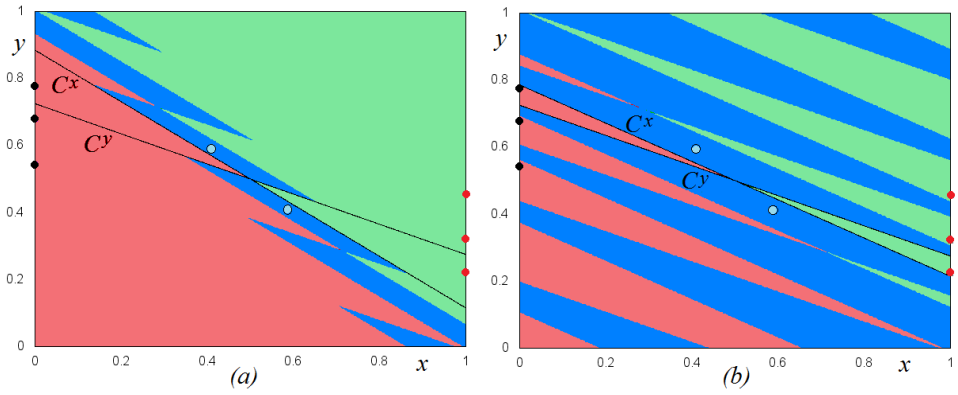

Figure 5: Case IV. Coexisting attracting interior 2-cycle and two border 3-cycles together with their basins. Here $\delta = 0.3$ and $(m_x, m_y) = (1.3, 0.45)$ in (a), $(m_x, m_y) = (1.75, 0.45)$ in (b), so that the (m_x, m_y)-parameter point is, respectively, below and above curve B given in (10).

Clearly, the appearance of an attracting internal cycle Γ_2 leads to a change in the basins of attraction of the cycles γ_n and γ'_n, moreover, these basins differ depending on the location of the (m_x, m_y)-parameter point

wrt curve B. Recall that for $(m_x, m_y) \in R_{III}$ the basins of γ_n and γ'_n are separated by the discontinuity line C^x. For $(m_x, m_y) \in R_{IV}$ with $m_y < \frac{1-\delta m_x}{m_x(1-\delta)}$, that is, if (m_x, m_y)-point is below the curve B, the basins of γ_n and γ'_n remain simply connected (see an example in Fig.5a where an interior 2-cycle coexists with two border 3-cycles). On the other hand, for $(m_x, m_y) \in R_{IV}$ with $m_y > \frac{1-\delta m_x}{m_x(1-\delta)}$, that is, if (m_x, m_y)-point is above the curve B, the basins of γ_n and γ'_n are disconnected in I^2 (an example is shown in Fig.5b). All the basins are separated by the proper segments of the discontinuity lines C^x, C^y and their preimages. It is worth to note also that curve B converges to curve C as $\delta \to 0$, that is, the subregion of R_{IV} associated with disconnected basins decreases and disappears as $\delta \to 0$.

In the transition from Case IV to Case V crossing the curve C given in (6), for example, increasing m_y for fixed $m_x > 1$ (see e.g., Fig.2), the discontinuity curves C^x and C^y are merging and switching their position wrt each other. As a result, in the parameter region above the curve C the cycles γ_n and γ'_n no longer exist (it can be shown that in a lower neighbourhood of the curve C only the basic cycles $\gamma_n \in I_0$ and $\gamma'_n \in I_1$, $n \geq 1$, with symbolic sequences $L^n R$ and $R^n L$, respectively, still exist), while new interior cycles may appear as we show in the next section.

6 Cases V, VI: Interior cycles and period incrementing structures

6.1 Border collision bifurcations of an interior cycle

Let us denote an interior cycle of map F as $\Gamma_{2n} = \{p_i\}_{i=0}^{2n-1} = \{(x_i, y_i)\}_{i=0}^{2n-1}$, $n \geq 1$. We represent such a cycle by a symbolic sequence $\sigma = \sigma_0\sigma_1...\sigma_{2n-1}$ where $\sigma_i \in \{1, 2, 3, 4\}$ and

$$\sigma_i = \begin{cases} 1 & \text{if } p_i \in D_1 \\ 2 & \text{if } p_i \in D_2 \\ 3 & \text{if } p_i \in D_3 \\ 4 & \text{if } p_i \in D_4 \end{cases}$$

Property 4. Let $(m_x, m_y) \in R_V \cup R_{VI}$. Any interior cycle Γ_{2n}, $n \geq 1$, of map F can be represented by the symbolic sequence $1^k 4^l 2^k 3^l$ where $k \geq 1$, $l \geq 0$. The period of Γ_{2n} can be written as $2n = 2(k + l)$.

To see this consider first an arbitrary initial point $q_0 = (x_0, y_0) \in D_1$. Applying map F_1 the trajectory moves along the straight line $y = \frac{y_0-1}{x_0}x + 1$ approaching the fixed point $(x, y) = (0, 1)$ of map F_1. Two cases can be distinguished:

(1) If after a number $i \geq 1$ of iterations by F_1 it holds that $q_i = F_1^i(q_0) \in D_2$ (this can occur if $(m_x, m_y) \in R_V$ and cannot occur if $(m_x, m_y) \in R_{VI}$), then applying F_2 the trajectory moves along the straight line $y = \frac{y_i}{x_i-1}(x - 1)$ towards the fixed point $(x, y) = (1, 0)$ of F_2. It is easy to see that the trajectory necessarily comes back to D_1 where F_1 is applied again. As a result, applying only the maps F_1 and F_2, the trajectory is attracted to the 2-cycle Γ_2 (see Property 3) which can be represented by the symbolic sequence $1^1 4^0 2^1 3^0$. Here the upper index 0 means that the related symbol is absent in the symbolic sequence. The parameter region defined by $m_x > 1$, $m_y < 1$, associated with Γ_2 is denoted $P_{0,1}$.

(2) If after a number $i \geq 1$ of iterations by F_1 it holds that $q_i = F_1^i(q_0) \in D_4$ (this can occur for $(m_x, m_y) \in R_V$ and necessarily occurs for $(m_x, m_y) \in R_{VI}$), then applying map F_4 the trajectory moves along the straight line $y = \frac{1-y_i}{1-x_i}x + 1$ towards the fixed point $(x, y) = (1, 1)$ of map F_4, and after a number $j \geq 1$ of iterations it necessarily enters region D_2, that is, $q_{i+j} = F_4^j \circ F_1^i(p_0) \in D_2$. Then, after a number of iterations by F_2 the trajectory enters region D_3, and applications by F_3 lead the trajectory back to region D_1. In such a way a cycle (of period at least 4) of map F may exist.

Consider a cycle $\Gamma_{2n} = \{p_i\}_{i=0}^{2n-1}$ of map F, $n \geq 2$, where p_0 is the rightmost periodic point in D_1. Then following the same reasoning as for a generic trajectory, we can state that there are numbers $k \geq 1$ and $l \geq 1$ such that $p_k = F_1^k(p_0) \in D_4$ and $p_{k+l} = F_4^l \circ F_1^k(p_0) \in D_2$. Due to the symmetry of F wrt S, point p_{k+l} is necessarily symmetric wrt S to point p_0, that is, it holds $p_{k+l} = (1-x_0, 1-y_0)$, and there are other $k-1$ points of Γ_{2n} in D_2 as well as l points in D_3, each of which is symmetric to the related point p_i, $1 \leq i \leq k + l - 1$. Thus, the cycle Γ_{2n} can be represented by the symbolic sequence $1^k 4^l 2^k 3^l$. We denote its existence region in the (m_x, m_y)-parameter plane as $P_{l,k}$. Two examples of Γ_{2n} are presented in Fig.6.

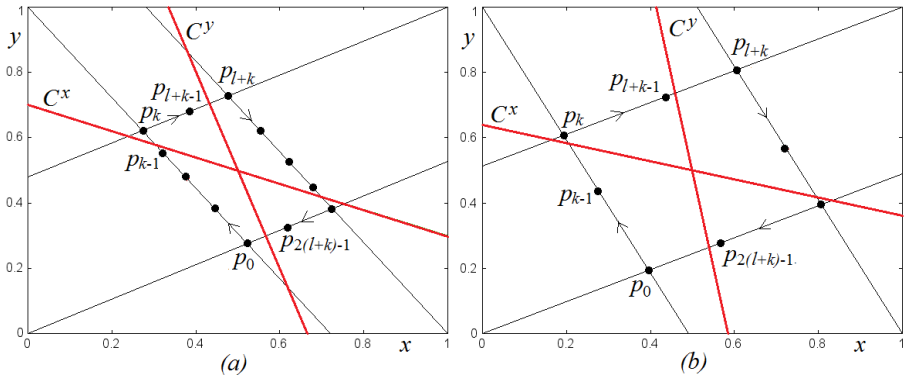

Figure 6: Examples of interior cycles $\Gamma_{2(k+l)} = \{p_i\}_{i=0}^{2(k+l)-1}$ of map F with k points in region D_1, l points in D_4, k points in region D_2 and l points in region D_3. In case (a) the related periodicity region $P_{l,k}$ has four boundaries, while in case (b) $P_{l,k}$ is unbounded on two sides (see Proposition 1).

Property 5. The rightmost point $p_0 \in D_1$ of the cycle $\Gamma_{2n} = \{p_i\}_{i=0}^{2n-1}$, $n \geq 1$, of map F with symbolic sequence $1^k 4^l 2^k 3^l$ has the following coordinates:

$$p_0 = (x_0, y_0) = \left(\frac{a^l}{1 + a^{l+k}}, \frac{a^{l+k}}{1 + a^{l+k}} \right), \quad a := 1 - \delta \tag{11}$$

To see this note that for $p_0 \in D_1$, where p_0 is the point of Γ_{2n} in D_1 with the largest x_0 coordinate, it holds

$$p_{k+l} = (a^l(a^k x_0 - 1) + 1, a^{l+k}(y_0 - 1) + 1)$$

then (11) follows from $p_{k+l} = (1 - x_0, 1 - y_0)$.

Proposition 1 *Let $0 < \delta < 1$, $a = 1 - \delta$, and $(m_x, m_y) \in R_V \cup R_{VI}$. Suppose map F has a cycle $\Gamma_{2n} = \{p_i\}_{i=0}^{2n-1}$, $n \geq 2$. Then it is an interior attracting cycle of period $2(k + l)$ with the symbolic sequence $1^k 4^l 2^k 3^l$, where $1 \leq l \leq \bar{l}$, $k \geq l$, and $\bar{l} = \lfloor \log_{1-\delta} 0.5 \rfloor + 1$. In the (m_x, m_y)-parameter plane the related periodicity region $P_{l,k}$ is confined by at most four boundaries associated with the border collision bifurcations of Γ_{2n}:*

$$B^1_{l,k}: \quad m_y = \frac{a^{l+k} - 1}{1 + a^l(a^k - 2)} =: m^1_{y(l,k)} \qquad (p_0 \in C^y) \tag{12}$$

$$B^2_{l,k}: \quad m_y = \frac{a^{l+k-1}(2 - a) - 1}{1 + a^{l-1}(a^{k+1} - 2)} =: m^2_{y(l,k)} \qquad (p_{2(k+l)-1} \in C^y) \tag{13}$$

$$B^3_{l,k}: \quad m_x = \frac{1 - a^{l+k}}{1 + a^k(a^l - 2)} =: m^3_{x(l,k)} \qquad (p_k \in C^x) \tag{14}$$

$$B^4_{l,k}: \quad m_x = \frac{1 - a^{l+k-1}(2 - a)}{1 + a^{k-1}(a^{l+1} - 2)} =: m^4_{x(l,k)} \qquad (p_{k-1} \in C^x) \tag{15}$$

The region $P_{l,k}$ can be one-side unbounded (only the boundaries $B^1_{l,k}$, $B^2_{l,k}$ and $B^3_{l,k}$, or $B^2_{l,k}$, $B^3_{l,k}$ and $B^4_{l,k}$, exist) or two-side unbounded (only the boundaries $B^2_{l,k}$ and $B^3_{l,k}$ exist).

Proof. Let $0 < \delta < 1$, $(m_x, m_y) \in R_V \cup R_{VI}$. Suppose that map F has a cycle $\Gamma_{2n} = \{p_i\}_{i=0}^{2n-1}$, $n \geq 1$. Then Γ_{2n} can be represented by the symbolic sequence $1^k 4^l 2^k 3^l$ (see Property 4), where $1 \leq l \leq \bar{l}$, $k \geq l$ (the value $\bar{l}$ is discussed in Proposition 2), and the rightmost point $p_0 \in D_1$ of Γ_{2n} has coordinates given in (11) (see Property 5).

Increasing m_y (the slope of the discontinuity line C^y given in (5) becomes larger in modulus, see Fig.7a) a BCB of Γ_{2n} can occur at which $p_0 \in C^y$. From the condition $p_0 \in C^y$ the boundary $B^1_{l,k}$ of $P_{l,k}$ is obtained (see Fig.7b). Obviously, such a BCB cannot occur if $x_0 \leq \frac{1}{2}$ (see Fig.6b) given that it must hold $m_y > 0$ (i.e., the slope of C^y must be negative). Thus, if $x_0 \leq \frac{1}{2}$, that is, if $1 + a^l(a^k - 2) \geq 0$, the boundary $B^1_{l,k}$ of $P_{l,k}$ does not exist and $P_{l,k}$ is at least one-side unbounded. Note that in such a case it holds that $m^1_{y(l,k)} < 0$.

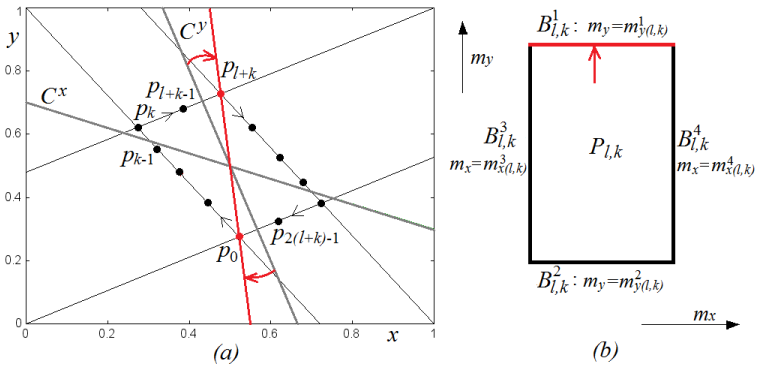

Figure 7: Approaching boundary $B^1_{l,k}$ of the periodicity region $P_{l,k}$ by increasing m_y: in (a) it is shown how the curve C^y moves, and in (b) the related boundary is indicated.

Decreasing m_y (the slope of C^y becomes smaller in modulus, see Fig.8a) a BCB of Γ_{2n} can occur at which $p_{2(k+l)-1} \in C^y$ where

$$p_{2(k+l)-1} = \left(\frac{a^{l-1}}{1+a^{l+k}}, \frac{a^{l+k-1}}{1+a^{l+k}} \right)$$

From the condition $p_{2(k+l)-1} \in C^y$ the boundary $B^2_{l,k}$ is obtained (see Fig.8b). It is easy to see that for the considered parameter values such a BCB always occurs, that is, the boundary $B^2_{l,k}$ of $P_{l,k}$ always exists.

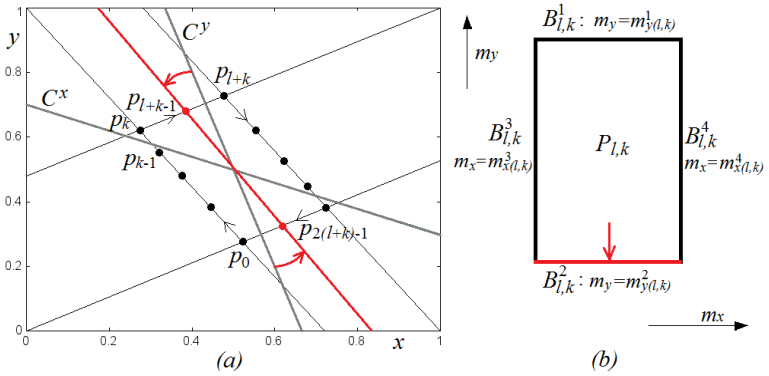

Figure 8: Approaching boundary $B^2_{l,k}$ of the periodicity region $P_{l,k}$ by decreasing m_y: in (a) it is shown how the curve C^y moves, and in (b) the related boundary is indicated.

Let now m_x be decreasing (the slope of the discontinuity line C^x defined in (5) becomes larger in modulus, see Fig.9a). Then a BCB of Γ_{2n} can occur at which $p_k \in C^x$ where

$$p_k = \left(\frac{a^{l+k}}{1+a^{l+k}}, \frac{1+a^k(a^l-1)}{1+a^{l+k}} \right)$$

The equation for $B^3_{l,k}$ is obtained from the condition $p_k \in C^x$ (Fig.9b). For the considered parameter values such a BCB always occurs so that the boundary $B^3_{l,k}$ of $P_{l,k}$ always exists.

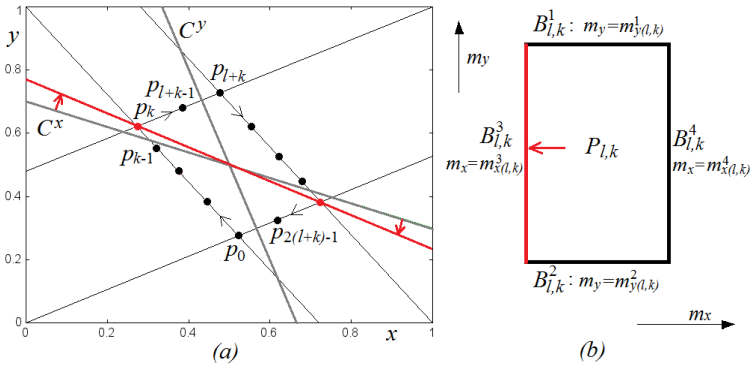

Figure 9: Approaching boundary $B^3_{l,k}$ of the periodicity region $P_{l,k}$ by decreasing m_x: in (a) it is shown how the curve C^x moves, and in (b) the related boundary is indicated.

Increasing m_x (the slope of C^x becomes smaller in modulus, see Fig.10a) a BCB of Γ_{2n} can occur at which $p_{k-1} \in C^x$ where

$$p_{k-1} = \left(\frac{a^{l+k-1}}{1+a^{l+k}}, \frac{1+a^{k-1}(a^{l+1}-1)}{1+a^{l+k}} \right)$$

The equation for $B^4_{l,k}$ is obtained from $p_{k-1} \in C^x$ (see Fig.10b). Such a BCB cannot occur if $y_{k-1} \leq \frac{1}{2}$ (see Fig.6b) given that it must hold $m_x > 0$ (i.e., the slope of C^x must be negative). Thus, if $y_{k-1} \leq \frac{1}{2}$, that is, if $1 + a^{k-1}(a^{l+1} - 2) \leq 0$, it holds that the boundary $B^4_{l,k}$ of $P_{l,k}$ does not exist and $P_{l,k}$ is at least one-side unbounded. Note that in such a case $m^4_{x(l,k)} < 0$ (in (15) the inequality $1 - a^{l+k-1}(2-a) > 0$ follows from $x_{l+k-1} < \frac{1}{2}$).

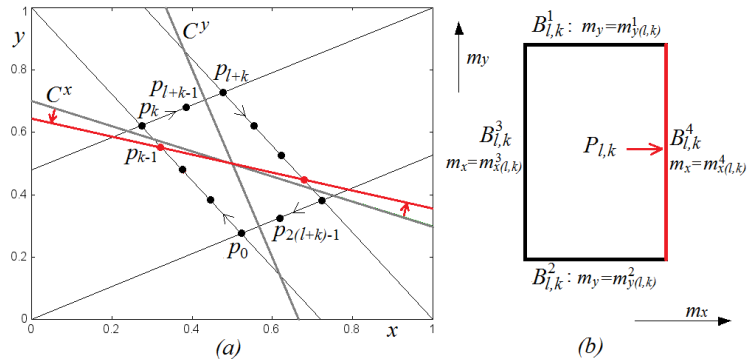

Figure 10: Approaching boundary $B^4_{l,k}$ of the periodicity region $P_{l,k}$ by increasing m_x: in (a) it is shown how the curve C^x moves, and in (b) the related boundary is indicated.

To summarize, if all the BCB values given in (12)-(15) are positive, it holds that $m^1_{y(l,k)} > m^2_{y(l,k)}$ and $m^4_{x(l,k)} > m^3_{x(l,k)}$, that is, $B^1_{l,k}$, $B^2_{l,k}$, $B^3_{l,k}$ and $B^4_{l,k}$ are, respectively, upper, lower, left and right boundaries of $P_{l.k}$. If for some values of k, l it holds that $m^1_{y(l,k)} < 0$ (i.e., $1 + a^l(a^k - 2) > 0$) then such a region is unbounded from above, while if $m^4_{x(l,k)} < 0$ (i.e., $1 + a^{k-1}(a^{l+1} - 2) < 0$) holds then the related region is unbounded from the right. ■

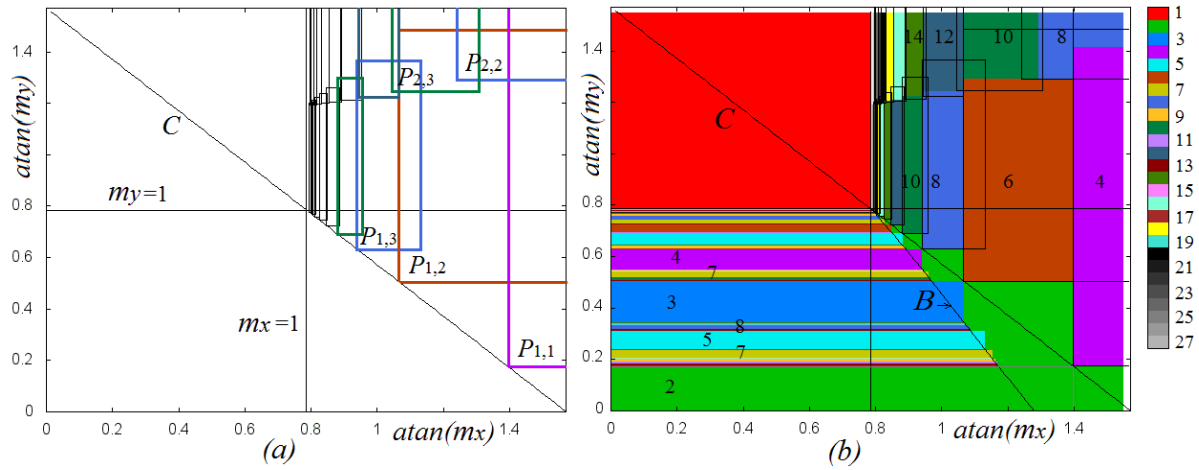

Figure 11: BCB boundaries of the periodicity regions $P_{l,k}$, $l = 1, 2$, $k \geq l$, in the $(\arctan(m_x), \arctan(m_y))$-parameter plane for $\delta = 0.3$.

6.2 Properties of the period incrementing structures

Fig.11a shows an example of the BCB boundaries confining the periodicity regions $P_{l,k}$ in the $(\arctan(m_x), \arctan(m_y))$-parameter plane for $\delta = 0.3$ (some boundaries are shown in color associated with the colliding cycle). As we show below (see Proposition 2), for such a value of δ it holds that $l \leq \bar{l} = 2$, that is, there are two sets of periodicity regions, $\{P_{1,k}\}_{k=1}^{\infty}$ and $\{P_{2,k}\}_{k=2}^{\infty}$, which are related to the cycles with symbolic sequences $1^k4^12^k3^1$ and $1^k4^22^k3^2$. In Fig.11b the BCB boundaries of the periodicity regions are superposed on the 2D bifurcation diagram obtained numerically. One can see that the regions $P_{1,k}$ and $P_{1,k+1}$, $k \geq 1$, are partially overlapping and for $k \to \infty$ they accumulate to $m_x = 1_+$. So, the set of regions $\{P_{1,k}\}_{k=1}^{\infty}$ form a period incrementing bifurcation structure with incrementing step 2. The same holds for regions $\{P_{2,k}\}_{k=2}^{\infty}$. Note that regions $P_{1,1}$ and $P_{2,2}$ are two side unbounded, $P_{1,2}$ is unbounded from the right and $P_{2,k}$, $k \geq 3$, are unbounded from above. Note also that the periodicity regions of different incrementing structures, that is, for $l = 1$ and $l = 2$, are also partially overlapping, so that more than 2 different cycles may coexist. An example of 4 coexisting cycles[11] is shown in Fig.12b, and the related parameter point is indicated in Fig.12a.

Proposition 2 *For a fixed $0 < \delta < 1$ the number of the period incrementing bifurcation structures in the (m_x, m_y)-parameter plane of map F is given by*

$$\bar{l} = \lfloor \log_{1-\delta} 0.5 \rfloor + 1 \tag{16}$$

that is, map F can have cycles with symbolic sequences $1^k4^l2^k3^l$ for any $1 \leq l \leq \bar{l}$ and $k \geq l$. Here $\lfloor \cdot \rfloor$ denotes the integer part of the number.

Proof. Suppose that $0 < \delta < 1$ is fixed and in the (m_x, m_y)-parameter plane of map F there is more than one period incrementing structure. Consider a set of periodicity regions $\{P_{l,k}\}_{k=l}^{\infty}$ for some fixed $l \geq 2$. For the boundaries of these regions, defined in (12)-(15), we have

$$\lim_{k\to\infty} m^3_{x(l,k)} = 1, \quad \lim_{k\to\infty} m^4_{x(l,k)} = 1$$

$$\lim_{k\to\infty} m^1_{y(l,k)} = \frac{1}{2(1-\delta)^l - 1} =: m_{y,l} \tag{17}$$

[11] As it follows from Proposition 2 the number of incrementing structures increases as $\delta \to 0$. Then more than 2 incrementing structures can overlap leading to more than 4 coexisting cycles.

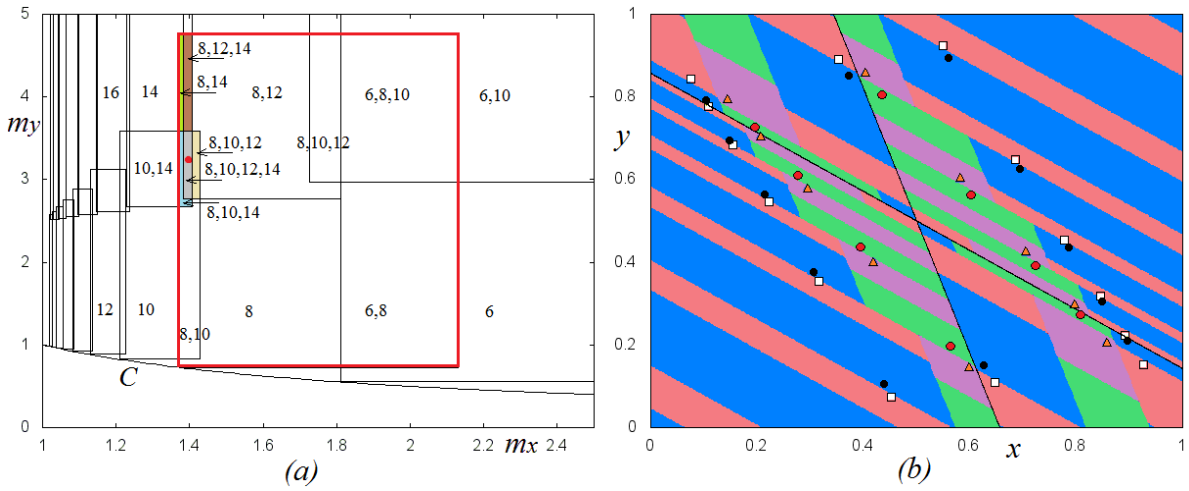

Figure 12: (a) BCB boundaries of the periodicity regions in the (m_x, m_y)-parameter plane for $\delta = 0.3$; some periods are indicated by numbers; (b) For $\delta = 0.3$, $m_x = 1.4$, $m_y = 3.2$ (the related point is indicated by red circle in (a)) in the phase plane there are coexisting 8-, 10-, 12- and 14-cycles with symbolic sequences $1^3 4^1 2^3 3^1$, $1^4 4^1 2^4 3^1$, $1^4 4^2 2^4 3^2$ and $1^5 4^2 2^5 3^2$, respectively.

$$\lim_{k\to\infty} m^2_{y(l,k)} = \frac{1}{2(1-\delta)^{l-1} - 1} = m_{y,l-1} \tag{18}$$

Since the convergence of the sequence $m^2_{y(l,k)}$ as $k \to \infty$ is monotone, $m^2_{y(l,k+1)} < m^2_{y(l,k)}$, it follows that if the sequence of lower boundaries $B^2_{l,k}$ of $P_{l,k}$ converges to a positive value, that is, if $m_{y,l-1} > 0$, the related set of periodicity regions, forming a period incrementing structure, exists. From the condition $m_{y,l-1} > 0$ we get that $l \le \bar{l} = \lfloor \log_{1-\delta} 0.5 \rfloor + 1$. ■

The next two properties follow immediately from (16):

Property 6. For $0.5 < \delta < 1$ it holds that $\bar{l} = 1$, i.e., in the (m_x, m_y)-parameter plane there is only one period incrementing structure formed by periodicity regions $P_{1,k}$, $k \ge 1$, unbounded from above (where $P_{1,1}$ is unbounded from the right side as well).

Property 7. As $\delta \to 0$ the number $\bar{l}$ of incrementing structures in the (m_x, m_y)-parameter plane tends to infinity.

As an example, Fig.13a presents the BCB boundaries for $\delta = 0.1$, and in Fig.13b they are superposed on the 2D bifurcation diagram obtained numerically. For such a value of δ there are $\bar{l} = 7$ period incrementing structures. For $\delta = 0.01$, for example, there are already $\bar{l} = 69$ period incrementing structures.

For the period incrementing structure $\{P_{1,k}\}_{k=1}^{\infty}$, $k \ge 1$, the following property can be verified by direct computation:

Property 8. In the (m_x, m_y)-parameter plane the vertex point $p^{2,3}_{1,k} := B^2_{1,k} \cap B^3_{1,k}$ of each region $P_{1,k}$, $k \ge 1$, given by $(m_x, m_y) = (m^3_{x(1,k)}, m^2_{y(1,k)})$, belongs to the curve C given in (6), that is, $m^2_{y(1,k)} = 1/m^3_{x(1,k)}$.

Let us consider now the vertex point $p^{1,3}_{l,k} := B^1_{l,k} \cap B^3_{l,k}$ of the periodicity region $P_{l,k}$, given by $(m_x, m_y) = (m^3_{x(l,k)}, m^1_{y(l,k)})$, when it exists. From Property 6 it follows that a necessary condition for the existence of such a point is $0 < \delta < 0.5$.

Property 9. In the (m_x, m_y)-parameter plane the vertex point $p^{1,3}_{l,k}$ of any periodicity region $P_{l,k}$, if it exists (i.e., if $1 + a^{k-1}(a^{l+1} - 2) > 0$), is located above the diagonal $m_y = m_x$.

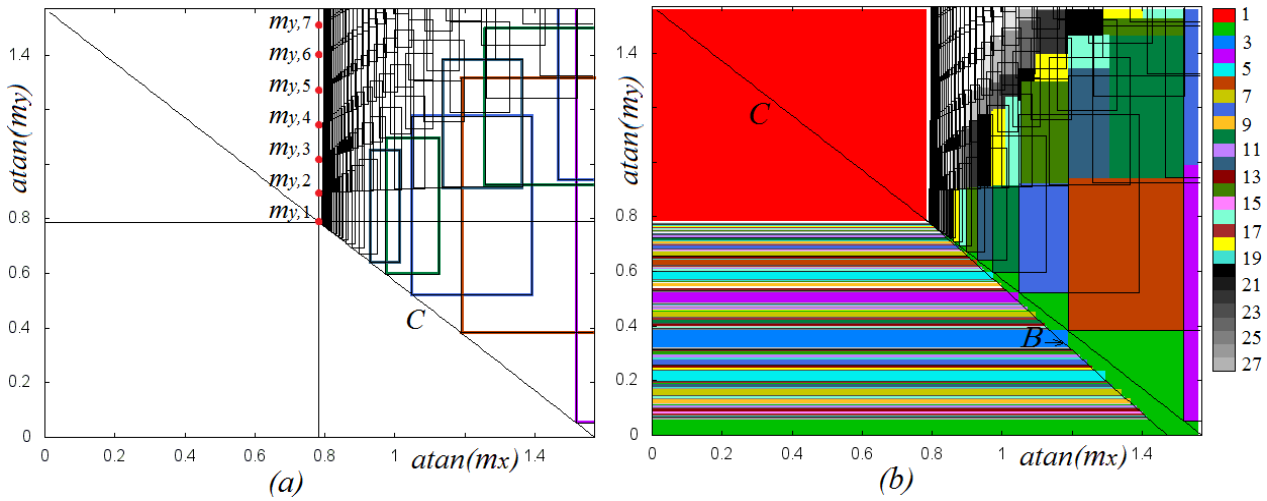

Figure 13: BCB boundaries of the periodicity regions $P_{l.k}$, $1 \le l \le 7$, $k \ge l$, in the $(\arctan(m_x), \arctan(m_y))$-parameter plane for $\delta = 0.1$.

A simple corollary of this property is that regions $P_{1,k}$, $k \ge 1$, extend from the parameter region R_V to the parameter region R_{VI}. Moreover, the following property holds:

Property 10. In the parameter region R_V there is only the period incrementing structure $\{P_{1,k}\}_{k=1}^{\infty}$ (extending to R_{VI}) which is overlapped by region $P_{0,1}$ related to 2-cycle Γ_2 (see Property 3).

To see this, note that for $0 < \delta < 0.5$ it holds that $m_{y,1} = \frac{1}{1-2\delta} > 1$, $m_{y,2} = 1$ (see (17), (18)) and for any $k \ge 2$ we have that $m^2_{y(2,k+1)} < m^2_{y(2,k)}$, that is, the period incrementing structure $\{P_{2,k}\}_{k=2}^{\infty}$ is located in R_{VI}.

The above property means that for $(m_x, m_y) \in R_V$ map F has an interior 2-cycle Γ_2 which may coexist or not with one cycle having symbolic sequence $1^k4^12^k3^1$, $k \ge 1$, or with two such cycles, with symbolic sequence $1^k4^12^k3^1$ and $1^{k+1}4^12^{k+1}3^1$. For example, in Fig.14a an interior 2-cycle coexists with 8-cycle $1^34^12^33^1$, and in Fig.14b it coexists with 6-cycle $1^24^12^23^1$ and 8-cycle $1^34^12^33^1$.

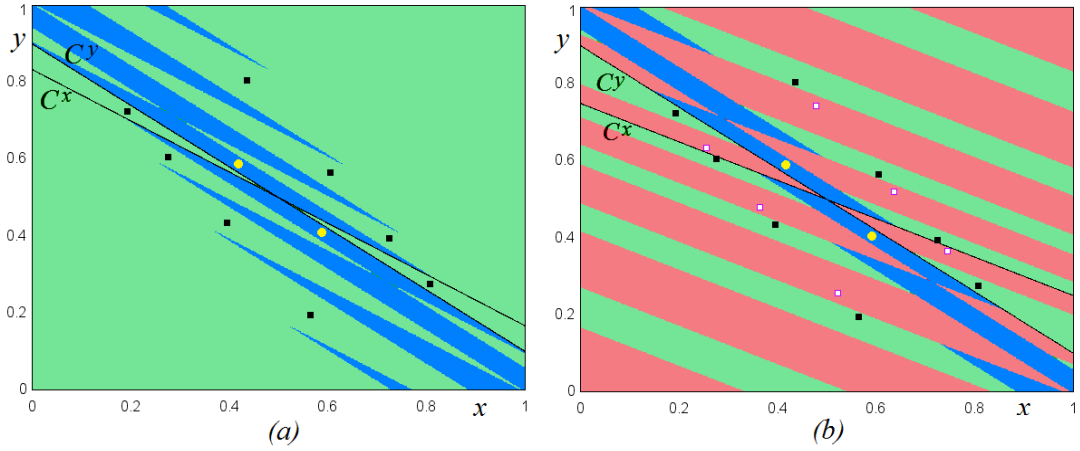

Figure 14: Coexisting interior 2- and 8-cycles in (a) and 2-, 6- and 8-cycles in (b), and their basins. Here $\delta = 0.3$, $m_y = 0.8$ and $m_x = 1.5$ in (a) and $m_x = 2$ in (b).

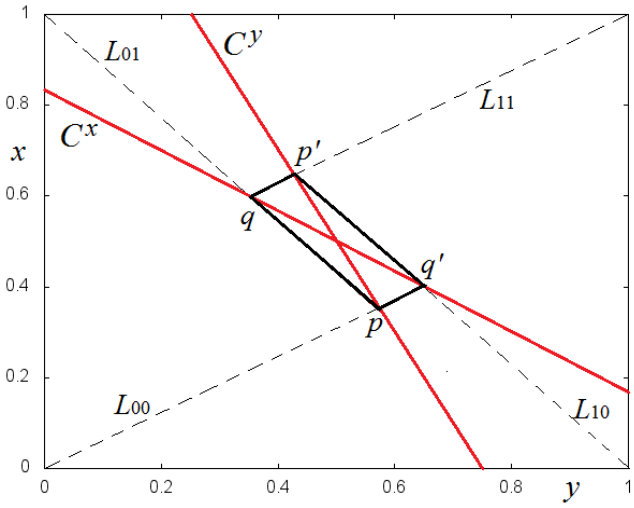

Figure 15: An example of parallelogram P with vertices given in (19) and (20), which can be constructed in the (x, y)-phase plane of map F for $m_y > m_x$, $m_x > 1$ and $0 < \delta < 1$.

6.3 Codimension-two BCB of an interior cycle

Consider a periodicity region $P_{l,k}$ and its vertex point $p_{l,k}^{1,3} = (m_{x(l,k)}^3, m_{y(l,k)}^2)$ (assuming that it exists, that is, $1 + a^{k-1}(a^{l+1} - 2) > 0$). In this section we describe the particular BCB of the related cycle $\Gamma_{2(l+k)}$, associated with such a parameter point.

We first construct for fixed $(m_x, m_y) \in R_V \cup R_{VI}$ an auxiliary parallelogram P in the (x, y)-phase plane (see an example in Fig.15), with vertices $p = (x_p, y_p) \in C^y$, $q = (x_q, y_q) \in C^x$, $p' = (x'_p, y'_p) \in C^y$, $q' = (x'_q, y'_q) \in C^x$ (where p' and q' are symmetric wrt S to p and q, respectively) and edges belonging to straight lines connecting point p (as well as q') with point $(0, 0)$, and q (as well as p) with $(0, 1)$. By symmetry, the other two edges belong to straight lines connecting p' (as well as q) with $(1, 1)$, and q' (as well as p') with $(1, 0)$. Recall that $(0, 0)$, $(0, 1)$, $(1, 1)$ and $(1, 0)$ are the fixed points of F_3, F_1, F_4 and F_2, respectively, which are virtual for F. The mentioned above straight lines are denoted, respectively, as L_{00}, L_{01}, L_{11} and L_{10} :

$$L_{00} : \quad y = \frac{y_p}{x_p} x, \qquad L_{01} : \quad y = \frac{y_q - 1}{x_q} x + 1$$
$$L_{11} : \quad y = \frac{y'_p - 1}{x'_p - 1}(x - 1) + 1, \qquad L_{10} : \quad y = \frac{y'_q}{x'_q - 1}(x - 1)$$

After some algebra one can get the coordinates of the vertices p, q, p' and q':

$$p = (x_p, y_p) = \left(\frac{1}{2} + \frac{M}{2m_y}, \frac{1}{2} - \frac{M}{2}\right), \quad q = (x_q, y_q) = \left(\frac{1}{2} - \frac{M}{2}, \frac{1}{2} + \frac{M}{2m_x}\right) \tag{19}$$

$$p' = (x'_p, y'_p) = \left(\frac{1}{2} - \frac{M}{2m_y}, \frac{1}{2} + \frac{M}{2}\right), \quad q' = (x'_q, y'_q) = \left(\frac{1}{2} + \frac{M}{2}, \frac{1}{2} - \frac{M}{2m_x}\right) \tag{20}$$

where

$$M = \frac{m_y - m_x}{m_x m_y - 1}$$

Note that by construction it must be $\frac{1}{2} < x_p < 1$ and $\frac{1}{2} < y_q < 1$, that is, the inequalities $0 < M < 1$, leading to $m_x > 1$, $m_x m_y > 1$ and $m_y > m_x$, have to be satisfied. The inequalities $m_x > 1$, $m_x m_y > 1$ are satisfied for the considered regions R_V and R_{VI}, thus, we can state the following

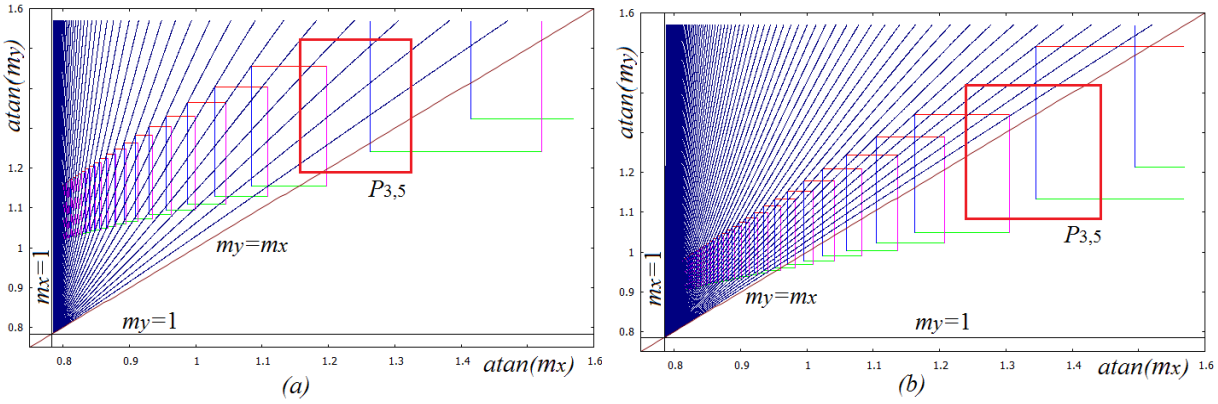

Figure 16: Period incrementing structure $\{P_{3,k}\}_{k=3}^{\infty}$ for $\delta = 0.1$ (a) and $\delta = 0.05$ (b). The curves V_k defined in (21), to which the vertex points $p_{l,k}^{1,3}$ belong, are shown for $1 \le k \le 100$. The region $P_{3,5}$ is highlighted.

Property 11. In the (x, y)-phase plane of map F a parallelogram P with vertices p, q, p' and q', given in (19) and (20), can be constructed if $m_y > m_x$, $m_x > 1$, independently on δ.

The following property can be verified by straightforward calculations:

Property 12. The vertex point $p_{l,k}^{1,3}$ of region $P_{l,k}$ is a codimension-2 BCB point at which four points of the cycle $\Gamma_{2(l+k)}$ collide with the borders: $p_0 = p \in C^y$, $p_k = q \in C^x$, $p_{k+l} = p' \in C^y$ and $p_{2k+l} = q' \in C^x$, where p, q, p' and q' are given in (19) and (20).

Recall that at the parameter point $p_{l,k}^{1,3}$ the inequality $m^1_{y(l,k)} > m^3_{x(l,k)}$ holds, thus, from Property 11 it follows that the parallelogram P can be constructed.

Note that from $p_0 = p$ it follows that points $p_{l,k}^{1,3}$ for different k belong to the curves

$$V_k: \qquad m_y = \frac{a^k m_x}{m_x(a^k - 1) + 1} \tag{21}$$

which for fixed k and $\delta \to 0$ (i.e., $a \to 1_-$) tend to the diagonal $m_y = m_x$, while for fixed δ and $k \to \infty$ tend to the vertical line $m_x = 1$. In Fig.16 the curves V_k are shown for $1 \le k \le 100$ and $\delta = 0.1$ in Fig.16a, $\delta = 0.05$ in Fig.16b.

It is interesting to note that as $m_x \to 1_+$, it holds that $p \to \left(\frac{m_y+1}{2m_y}, 0\right)$, $q \to (0, 1)$, $p' \to \left(\frac{m_y-1}{2m_y}, 1\right)$ and $q' \to (1, 0)$ (see (19) and (20)). We can formulate the following

Property 13. Let $m_y > 1$ and $0 < \delta < 1$ be fixed and $m_x \to 1_+$. Then for interior cycles $\Gamma_{2(l+k)}$ it holds that $k \to \infty$ and points p_{k-1} and p_k tend to $(0, 1)$, while the symmetric points $p'_{k-1} = p_{2k+l-1}$ and $p'_k = p_{2k+l}$ tend to $(1, 0)$. Crossing the boundary $m_x = 1$ (so that the (m_x, m_y) parameter point enters region R_I) leads to the attracting fixed points $(x, y) = (0, 1)$ and $(x, y) = (1, 0)$.

Proposition 3 *Let $0 < \delta < 1$, $m_y > m_x$ and $m_x > 1$. Then in the generic case any initial point (x_0, y_0) is attracted to a cycle Γ_{2n}, $n \ge 2$, of map F, and points of this cycle are external to the parallelogram P with vertices p, q, p' and q', given in (19) and (20).*

Proof. Generic case here means that the (m_x, m_y)-parameter point does not belong to a BCB boundary of some periodicity region. To prove this statement let us consider a non-generic case related to the parameter point $p_{l,k}^{1,3}$ at which $p_0 \in C^y$ and $p_k \in C^x$ and $p_0 = p$, $p_k = q$ (see Property 9). Then increasing m_x and decreasing m_y (so that the parameter point enters the region $P_{l,k}$) the points of the cycle $\Gamma_{2(l+k)}$ remain unchanged because their coordinates do not depend on m_x, m_y, while the vertices of parallelogram P move towards point S : it is

easy to check that for increasing m_x and decreasing m_y the value y_p increases, thus, the value x_p decreases, so that the vertex p becomes closer to S, and the same conclusion holds also for the other vertices of P. Thus, the points of the cycle, when it exists (i.e., for $(m_x, m_y) \in P_{l,k}$), cannot be located inside parallelogram P (recall that parallelogram P shrinks to point S for $m_y = m_x$, and does not exist for $m_y < m_x$). ■

7 Discrete versus continuous time model: a comparison of dynamics

As we already mentioned map F given in (4) describes the dynamics of a discrete-time version of the continuous-time fashion cycle model Λ given in (1). In the present section we show that the dynamics of map F as $\delta \to 0$ converge to those of the original continuous-time model. Recall that the discrete-time and continuous-time versions are related via $1 - \delta = e^{-\alpha \triangle}$, and $\delta \to 0$ as $\triangle \to 0$, where $\triangle$ is the time-delay in the discrete time formulation.

Similar to the partitioning of the (m_x, m_y)-parameter plane of the discrete-time model, the (m, m^*)-parameter plane of the continuous-time model Λ can be subdivided into six regions according to the location of the discontinuity lines $P_t = 0$ and $P_t^* = 0$: Case I ($m < 1 < mm^*$), Case II ($m < mm^* < 1$), Case III ($mm^* < m < 1$), Case IV ($m > 1 > mm^*$), Case V ($m > mm^* > 1$) and Case VI ($mm^* > m > 1$). The last case is further divided in Case VIa ($m \geq m^* > 1$) and Case VIb ($m^* > m > 1$). In the center of Fig.17 we show the corresponding partitioning of the (m, m^*)-parameter plane and around the center the corresponding dynamics are illustrated.

The description of possible attractors of the system Λ is summarized in

Proposition 4 ***[12]*** *The attractors of system Λ defined in (1) depending on parameters m and m^* are given by*

(a) $(\lambda_t, \lambda_t^*) = (0, 1)$ and $(\lambda_t, \lambda_t^*) = (1, 0)$ if $m^* > 1$, $m < 1$ (Cases I and II);
(b) $(\lambda_t, \lambda_t^*) = \left(0, \frac{1+m^*}{2}\right)$ and $(\lambda_t, \lambda_t^*) = \left(1, \frac{1-m^*}{2}\right)$ if $m^* < 1$, $mm^* < 1$ (Cases III and IV);
(c) $(\lambda_t, \lambda_t^*) = \left(\frac{1}{2}, \frac{1}{2}\right)$ if $\frac{1}{m} < m^* \leq m$ (Cases V and VIa);
(d) a limit cycle which is parallelogram L defined by vertices

$$P = \left(\frac{1}{2} + \frac{X_\infty}{2m^*}, \frac{1}{2} - \frac{X_\infty}{2}\right), \quad Q = \left(\frac{1}{2} - \frac{X_\infty}{2}, \frac{1}{2} + \frac{X_\infty}{2m}\right) \tag{22}$$

$$P' = \left(\frac{1}{2} - \frac{X_\infty}{2m^*}, \frac{1}{2} + \frac{X_\infty}{2}\right), \quad Q = \left(\frac{1}{2} + \frac{X_\infty}{2}, \frac{1}{2} - \frac{X_\infty}{2m}\right) \tag{23}$$

where

$$X_\infty = \frac{m^* - m}{mm^* - 1}$$

if $m^* > m > 1$ (Case VIb).

Comparing the dynamics of the discrete- and continuous-time fashion cycle models we can state the following

Proposition 5 *For $\delta \to 0$ the dynamics of the discrete-time fashion cycle model defined by map F given in (4) converges to the dynamics of the continuous-time fashion cycle model defined by the system Λ given in (1).*

Proof. In Cases I and II both models are associated with attracting border fixed points $(0, 1)$ and $(1, 0)$.

For Cases III and IV first note that the border cycles γ_n and γ'_n of map F belong to the intervals $J = [g_R(c), g_L(c)] \subset I_0$ and $J' = [g_R(c'), g_L(c')] \subset I_1$, respectively. It is easy to see that as $\delta \to 0$ intervals J and J' shrink to the discontinuity points $\left(0, \frac{1+m_y}{2}\right)$ and $\left(1, \frac{1-m_y}{2}\right)$, respectively, so that the border cycles γ_n and γ'_n also shrink to these points. Moreover, the interior 2-cycle $\Gamma_2 = \{p_0, p_1\}$ (see (9)) existing in the parameter region R_{IV} and R_V (Cases IV and V), shrinks to point S as $\delta \to 0$ (recall that point S is defined by $(x, y) = \left(\frac{1}{2}, \frac{1}{2}\right)$). It can be shown that in Case IV the basin of attraction of Γ_2 also shrinks. Thus, in Cases III and IV there is a correspondence of attractors of F as $\delta \to 0$ with those of system Λ (see item (b) of Proposition 4).

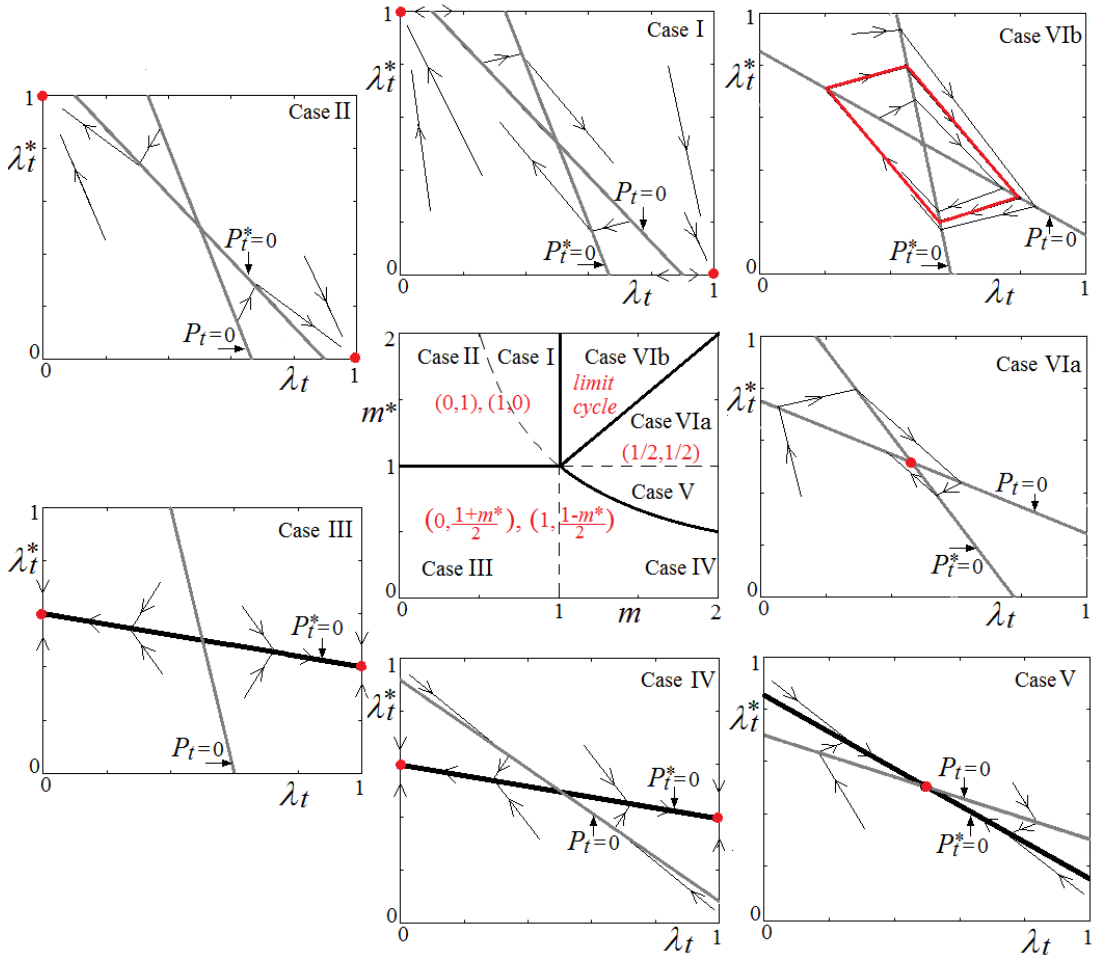

Figure 17: In the center: Partitioning of the (m, m^*)-parameter plane into the regions associated with different cases of continuous time fashin cycle model Λ. Around the center: The (λ_t, λ_t^*)-phase plane where examples of the discontinuity lines and attractors, corresponding to these regions, are shown.

In Case VI for $m_y \le m_x$, as well as in Case V, i.e., for the (m_x, m_y)-parameter point satisfying $\frac{1}{m_x} \le m_y \le m_x$, the trajectories of map F as $\delta \to 0$ tend to point S, as illustrated by the 1D bifurcation diagrams δ versus x for $m_y = 2$ and $m_x = 3$ in Fig.18a, and $m_y = m_x = 2$ in Fig.18b. Recall that map F can have coexisting cycles, and some of them are shown in Fig.18 by different colors. As one can see, for decreasing δ points of each cycle, as long as this cycle exists, tend to S, however, such a cycle may disappear due to a BCB.

In fact, let $0 < \delta < 1$ be fixed. Consider a parameter point (m_x, m_y) satisfying $\frac{1}{m_x} \le m_y \le m_x$. Such a point necessarily belongs to one or several (overlapping) periodicity regions. Let $(m_x, m_y) \in P_{l,k}$, then map F has the cycle $\Gamma_{2(l+k)}$ with point $p_0 \in D_1$ defined in (11). From (11) it follows that decreasing δ the point p_0 (as well as any other point of $\Gamma_{2(l+k)}$) tends to S. In the meantime, decreasing δ the value $m^1_{y(l,k)}$ (related to the BCB boundary $B^1_{l,k}$) decreases and the value $m^3_{x(l,k)}$ (related to $B^3_{l,k}$) increases, that can be verified using (21). It is illustrated in Fig.16, where the region $P_{3,5}$ is highlighted for $\delta = 0.1$ in Fig.16a and $\delta = 0.05$ in Fig.16b. Thus, decreasing δ cycle $\Gamma_{2(l+k)}$ either shrinks to S, or disappears due to a BCB colliding either with C^y (if boundary $B^1_{l,k}$ is crossed) or with C^x (if $B^3_{l,k}$ is crossed). Given that for each fixed $m_y \le m_x$ and decreasing δ the period of cycles of map F may increase but it remains finite (i.e., l and k in (11) do not tend to infinity), it holds that in the considered case the limit sets of the trajectories of F shrink to S, i.e., there is a correspondence

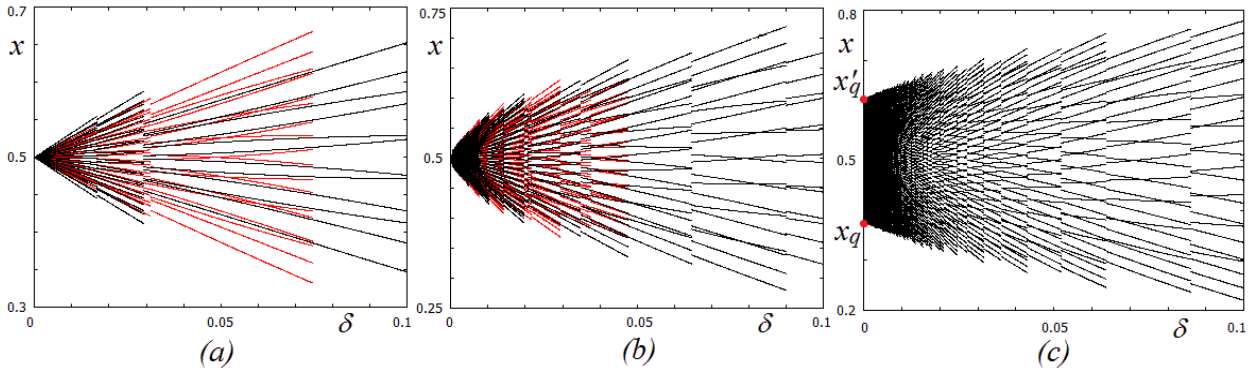

Figure 18: 1D bifurcation diagram δ versus x of map F for $0 < \delta < 0.1$, $m_y = 2$ and (a) $m_x = 3$, (b) $m_x = 2$, (c) $m_x = 1.5$.

with item (c) of Proposition 4.

In Case VI for $m_y > m_x$ the trajectories of map F as $\delta \to 0$ tend to cycles whose period tends to infinity and whose location tends to the parallelogram P with vertices defined in (19), (20) (note that these vertices correspond to those defined in (22), (23)). This case is illustrated in Fig.18c, where the 1D bifurcation diagram δ versus x is shown for $m_y = 2$ and $m_x = 1.5$. Here the points x_q and x'_q which are x-coordinates of the vertices q and q' of P, are also indicated. Note that for $m_x \to 1_+$ it holds that $x_q \to 0$ and $x'_q \to 1$.

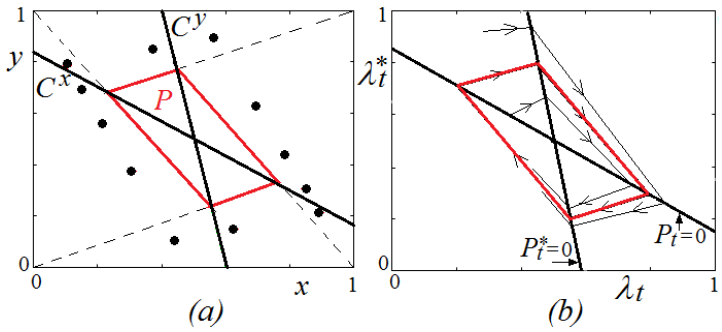

Figure 19: (a) In Case VI for $m_y > m_x$ and $\delta \to 0$ limit sets of trajectories of map F tend to parallelogram P; (b) the related parallelogram and convergence to it in the continuous-time fashion cycle model.

In fact, similarly to the previous case, for fixed $(m_x, m_y) \in P_{l,k}$ (with $m_y > m_x$) and decreasing δ the points of the related cycle $\Gamma_{2(l+k)}$ tend to S, however, $\Gamma_{2(l+k)}$ necessarily disappears due to a BCB colliding either with C^y when the boundary $B^1_{l,k}$ is crossed, or with C^x when $B^3_{l,k}$ is crossed (recall that as $\delta \to 0$ the point $p^{1,3}_{l,k}$ tends to the diagonal $m_y = m_x$, with decreasing $m^1_{y(l,k)}$ and increasing $m^3_{x(l,k)}$). Each new cycle which appears for decreasing δ has a higher period, moreover, according to Proposition 3, any cycle of map F remains external to the parallelogram P (recall that its vertices do not depend on δ). Thus, parallelogram P is a limit set for the trajectories of map F as $\delta \to 0$, which corresponds to item (d) of Proposition 4 (see Fig.19 where one can compare the parallelograms and trajectories of discrete- and continuous-time models in Case VIb). ■

8 Concluding remarks

We considered a 2D piecewise linear discontinuous map F depending on three parameters, which is a discrete-time version of the continuous-time fashion cycle model introduced in [12]. The map is chartarized by attracting cycles of different periods, with possible coexistence. Our objective was twofold: to describe the bifurcation structure of the parameter space of map F and to compare the obtained results with those associated with the continuous-time model. In fact, the bifurcation structure of map F is quite interesting: it is formed by the periodicity regions of attracting cycles organized in the period adding and period incrementing bifurcation structures. Recall that these structures are known to be characteristic for 1D piecewise monotone maps with one discontinuity point. In map F the period adding structure is standard being observed when map F is reduced to a 1D piecewise linear map. As for the period incrementing structure, it is related to the 2D dynamics and associated with the following peculiarities: if the coefficient of the contraction of the linear maps defining F is larger than $1/2$ then several partially overlapping period incrementing structures are observed, moreover, their number goes to infinity if the contraction coefficient tends to 1 (that corresponds also to the time-delay in the discrete time formulation of the model tending to zero). This leads, in particular, to more than two coexisting attracting cycles whose basin boundaries are formed by proper segments of discontinuity lines and their preimages. The rather simple analytical representation of map F allowed us to get the boundaries of all the periodicity regions in explicit form. We showed also that the dynamics of map F converges to the dynamics of its continuous-time counterpart if the time-delay in the discrete time formulation of the model tends to zero.

The question arises to which extent the considered fashion cycle model can be generalized. One possible direction is to break the symmetry of map F. Recall that in the present formulation the map is symmetric wrt the point $(x, y) = (1/2, 1/2)$ which is the intersection point of two discontinuity lines. We expect that if this point is no longer in the center of the unit square, the overall bifurcation structure will be only quantitatively modified. However, a definite answer to this question requires further research. It is also interesting to investigate the conditions for the existence of multiple overlapping period incrementing structures in a generic 2D piecewise linear map with one or two discontinuity lines.

ACKNOWLEDGMENTS

All the authors are grateful to the organizers and participants of Nonlinear Economic Dynamics Conference (Pisa, Sept. 7-9, 2017) for useful discussions which helped to improve the present work. The work of L. Gardini has been done within the activities of the GNFM (National Group of Mathematical Physics, INDAM Italian Research Group). I. Sushko thanks the University of Urbino for the hospitality experienced during her stay there as a Visiting Professor. K. Matsuyama is also grateful to the University of Urbino for the hospitality during his visit.

APPENDIX

The *period adding bifurcation structure*, also known as *Arnold tongues* or *mode-locking tongues*, is characteristic for a certain class of circle maps, for discontinuous maps defined by two increasing functions, for nonlinear maps undergoing Neimark-Sacker bifurcation, etc. (see, e.g. [9], [8], [4], [5]). The periodicity regions forming this structure in the parameter space of map F given in (4) are associated with attracting n-cycles, $n \geq 2$, of the 1D piecewise linear discontinuous map g given in (7) defined on the left border of I^2 (as well as with the symmetric n-cycles of map g' defined on the right border of I^2). Recall that for $0 < \delta < 1$ and $m_y < 1$, $m_x < 1$ (Case III) the left and right borders of I^2 are invariant, and map F on these borders is reduced on the 1D maps g and g', respectively. Given that dynamics of these maps are symmetric to each other wrt points S, below we consider the dynamics of map g only.

To describe the period adding structure we first need to introduce the symbolic representation of a cycle. The two partitions, $0 < y < c$ and $c < y < 1$ where $c = (m_y + 1)/2$, in which two linear branches of map g (with slopes $a = 1 - \delta < 1$) are defined, are associated with symbols L and R. Using these symbols any generic n-cycle $\{y_i\}_0^{n-1}$ of map g can be represented by a symbolic sequence $\sigma = \sigma_0\sigma_1...\sigma_{n-1}$, $\sigma_i \in \{L, R\}$, where $\sigma_i = L$ if $y_i \in L$ and $\sigma_i = R$ if $y_i \in R$. The rotation number of the n-cycle can be defined as m/n, where n is the number of points of the cycle (i.e., its period) and m is the number of points in the right partition. The periodicity regions forming the period adding structure are related to cycles with different rotation numbers.

These regions are ordered in the parameter space according to the *Farey summation rule* applied to the rotation numbers of the related cycles, namely, between the regions corresponding to the cycles with rotation numbers m_1/n_1 and m_2/n_2 (which are Farey neighbors) there is a region related to the cycle with rotation number $(m_1+m_2)/(n_1+n_2)$.

A more generic definition of the rotation number is given as

$$\rho(y) = \lim_{n\to\infty} \frac{1}{n} \sum_{k=0}^{n} \chi_r(g^k(y))$$

where χ_r is the characteristic function of the right partition:

$$\chi_r(y) = \begin{cases} 0 & \text{if } 0 < y < c \\ 1 & \text{if } c < y < 1 \end{cases}$$

For map g the rotation number is the same for any point y, $\rho(y) := \rho$. If ρ is a rational number, the above definition coincides with the one given for a cycle, while if ρ is an irrational number then map g has a Cantor set attractor (represented by the closure of quasiperiodic trajectories). Such an attractor is not persistent under parameter perturbations.

To get the boundaries of the periodicity regions analytically, all the cycles associated with the period adding structure are first grouped into certain families, called *complexity levels* (see [9], [1], [5]). For the sake of simplicity we denote a cycle by its symbolic sequence. The *complexity level one* includes two families of basic cycles:

$$C_{1,1} = \{LR^{n_1}\}_{n_1=1}^{\infty}, \quad C_{2,1} = \{RL^{n_1}\}_{n_1=1}^{\infty} \tag{24}$$

Recall that any n-cycle of map g is always attracting, with multiplier $\lambda = a^n < 1$. Thus, its periodicity region can be confined only by the boundaries related to the BCBs. In fact, there are two boundaries: if the parameter point crosses one boundary then a periodic point, which is nearest from the left to the discontinuity point $y = c$, collides with it, and crossing the other boundary a point of the cycle, which is nearest from the right to $y = c$, collides with this discontinuity point. In order to obtain analytical expressions of these boundaries it is convenient to shift the discontinuity point of map g to the origin, introducing the new variable $x := y - c$. In such a way we obtain a topologically conjugate map

$$\widetilde{g} : x \to \widetilde{g}(x) = \begin{cases} \widetilde{g}_L(x) = ax + \delta(1-c), & -c \le x < 0 \\ \widetilde{g}_R(x) = ax - \delta c, & 0 < x \le 1-c \end{cases} \tag{25}$$

Using the BCB conditions mentioned above and coordinates of the corresponding periodic points, one can obtain the boundaries of the periodicity region $P_{LR^{n_1}}$ related to the basic cycle LR^{n_1}, $n_1 \ge 1$:

$$\begin{aligned} \phi^L_{LR^{n_1}} &= \left\{(\delta, m_y) : 0 < \delta < 1,\ m_y = \frac{2(a^{n_1}-1)}{1-a^{n_1+1}} + 1\right\} \\ \phi^R_{LR^{n_1}} &= \left\{(\delta, m_y) : 0 < \delta < 1,\ m_y = \frac{2\delta a^{n_1-1}}{1-a^{n_1+1}} - 1\right\} \end{aligned}$$

Similarly, the boundaries of the periodicity region $P_{RL^{n_1}}$ related to the basic cycle RL^{n_1} can be obtained:

$$\begin{aligned} \phi^R_{RL^{n_1}} &= \left\{(\delta, m_y) : 0 < \delta < 1,\ m_y = -\frac{2(a^{n_1}-1)}{1-a^{n_1+1}} - 1\right\} \\ \phi^L_{RL^{n_1}} &= \left\{(\delta, m_y) : 0 < \delta < 1,\ m_y = -\frac{2\delta a^{n_1-1}}{1-a^{n_1+1}} + 1\right\} \end{aligned}$$

For example, for $n_1 = 1$, i.e., for the basic 2-cycle RL (which is the unique basic cycle belonging to both families $C_{1,1}$ and $C_{2,1}$) the related region P_{RL} is bounded by the curves

$$\phi_{LR} = \left\{(\delta, m_y) : 0 < \delta < 1,\ m_y = -\frac{\delta}{2-\delta}\right\}$$

$$\phi_{RL} = \left\{ (\delta, m_y) : 0 < \delta < 1,\ m_y = \frac{\delta}{2-\delta} \right\}$$

Note that in the (δ, m_y)-parameter plane the curves $\phi^L_{LR^{n_1}}$ and $\phi^R_{RL^{n_1}}$, as well as $\phi^R_{LR^{n_1}}$ and $\phi^L_{RL^{n_1}}$, are symmetric wrt the axis $m_y = 0$.

Recall that the feasible parameter range for the considered fashion cycle model is $m_y > 0$, thus, map g has only basic cycles associated with the family $C_{2,1}$, i.e., with cycles RL^{n_1}. In the meantime for the symmetric map g' the same periodicity regions correspond to the basic cycles related to the family $C_{1,1}$, i.e., to cycles LR^{n_1}. In Fig.20 the boundaries of regions$P_{RL^{n_1}}$ and $P_{LR^{n_1}}$ are shown in black for $1 \le n_1 \le 50$ in the (δ, c)- and (δ, c')-parameter planes, respectively, where $c = (1 + m_y)/2$ is the discontinuity point of map g and $c' = 1 - c = (1 - m_y)/2$ is the discontinuity point of map g'.

In the (m_x, m_y)-parameter plane the boundaries $\phi^L_{RL^{n_1}}$ for $n_1 \ge 2$ and $\phi^R_{RL^{n_1}}$ for $n_1 \ge 1$ (which are represented by the horizontal straight lines) extend from region R_{III} to region R_{IV} (see, e.g., Fig.2) up to the curve B defined in (10). Above this curve each region $P_{RL^{n_1}}$ has no lower boundary while new vertical boundary appears defined by a collision of the rightmost point of cycle RL^{n_1} with the discontinuity point d given in (8):

$$\psi_{RL^{n_1}} = \left\{ (m_x, m_y) : m_x = \frac{1 - a^{n_1+1}}{1 - a^{n_1}(2-a)},\ 1 + \frac{1 - m_x}{a m_x} < m_y < \frac{1}{m_x} \right\}$$

In the gaps between the periodicity regions $P_{LR^{n_1}}$ and $P_{LR^{n_1+1}}$, as well as $P_{RL^{n_1}}$ and $P_{RL^{n_1+1}}$, related to the cycles of the first complexity level (i.e., basic cycles), the periodicity regions associated with the families of higher complexity levels are located. In order to get the boundaries of these regions we first construct for each gap a corresponding first return map in a proper neighbourhood of the discontinuity point. This map appears to be of the same class of maps as the original one. Thus, for each first return map we can repeat the same reasoning as for the original map and get the boundaries of the periodicity regions related to the basic cycles. For the original map these cycles are associated with 2^2 families of the *complexity level two:*

$$C_{1,2} = \{LR^{n_1}\,(RLR^{n_1})^{n_2}\}^{\infty}_{n_1,n_2=1}\,, \quad C_{2,2} = \{RLR^{n_1}\,(LR^{n_1})^{n_2}\}^{\infty}_{n_1,n_2=1}$$

$$C_{3,2} = \{RL^{n_1}\,(LRL^{n_1})^{n_2}\}^{\infty}_{n_1,n_2=1}\,, \quad C_{4,2} = \{LRL^{n_1}\,(RL^{n_1})^{n_2}\}^{\infty}_{n_1,n_2=1}$$

and the boundaries of the corresponding periodicity regions are given as

$$\phi^L_{C_{1,2}} = \left\{ (\delta, m_y) : 0 < \delta < 1,\ m_y = \frac{2\delta a^{n_1}(1 - a^{(n_1+2)(n_2+1)})}{(1 - a^{n_1+2})(1 - a^{n_1+1+n_2(n_1+2)})} - 1 \right\}$$

$$\phi^R_{C_{1,2}} = \left\{ (\delta, m_y) : 0 < \delta < 1,\ m_y = -\frac{2\delta a^{n_1}(a^{n_2(2+n_1)-1}(a^{n_1+2} - \delta) - 1)}{(1 - a^{n_1+2})(1 - a^{n_1+1+n_2(n_1+2)})} - 1 \right\}$$

$$\phi^L_{C_{2,2}} = \left\{ (\delta, m_y) : 0 < \delta < 1,\ m_y = \frac{2\delta a^{n_1}(1 - a^{(n_1+1)(1+n_2)})}{(1 - a^{n_1+1})(1 - a^{n_1+2+n_2(n_1+1)})} - 1 \right\}$$

$$\phi^R_{C_{2,2}} = \left\{ (\delta, m_y) : 0 < \delta < 1,\ m_y = \frac{2a^{n_1}\delta(1 - a^{n_2(1+n_1)}(a^{n_1+2} + \delta))}{(1 - a^{n_1+1})(1 - a^{n_1+2+n_2(n_1+1)})} - 1 \right\}$$

The other four boundaries are symmetric wrt $m_y = 0$, namely, $\phi^L_{C_{3,2}}$ is symmetric to $\phi^R_{C_{1,2}}$, $\phi^R_{C_{3,2}}$ to $\phi^L_{C_{1,2}}$, $\phi^L_{C_{4,3}}$ to $\phi^R_{C_{2,2}}$ and, finally, $\phi^R_{C_{4,3}}$ to $\phi^L_{C_{2,2}}$. In Fig.20 these boundaries are shown in red for $1 \le n_1 \le 50$, $1 \le n_2 \le 10$, in the (δ, c)-parameter plane for map g and in the (δ, c')-parameter plane for map g'.

Reasoning in a similar way regarding the gaps between the regions of the complexity level two one can get 2^3 families of the *complexity level three* and the boundaries of the corresponding periodicity regions. This process can be continued *ad infinitum*. For more details see [1], [5] and references therein.

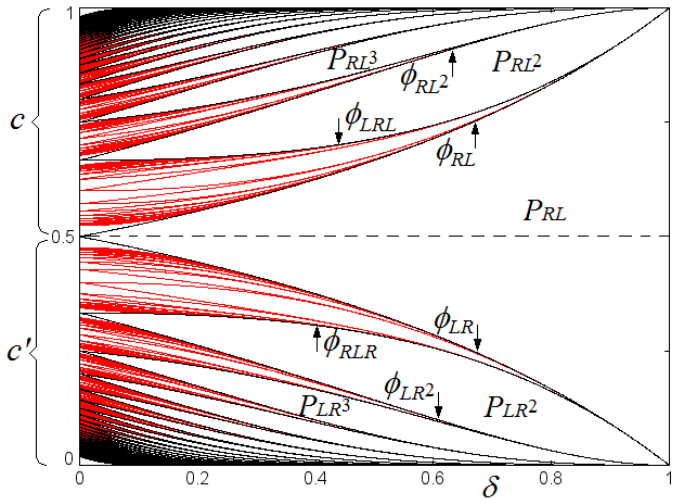

Figure 20: The period adding structure of map g given in (7) in the (δ, c)-parameter plane, and of map g' (symmetric to g) in the (δ, c')-parameter plane, where $c = (1 + m_y)/2$ and $c' = 1 - c = (1 - m_y)/2$ are the discontinuity points of g and g', respectively. Here the boundaries of the periodicity regions associated with cycles of complexity level one and two are shown in black and red, respectively.

References

[1] Avrutin V., Schanz M. & Gardini L. (2010). Calculation of bifurcation curves by map replacement. *Int. J. Bif. Chaos*, **20**, 3105-3135.

[2] Avrutin V., Sushko I. A gallery of bifurcation scenarios in piecewise smooth 1D maps. In: Global analysis of dynamic models for economics, finance and social sciences (G.-I. Bischi, C. Chiarella and I. Sushko Eds.), Springer, 2013.

[3] M. di Bernardo, C.J. Budd, A.R. Champneys, and P. Kowalczyk, Piecewise-smooth Dynamical Systems: Theory and Applications, Applied Mathematical Sciences 163, Springer, 2008.

[4] Boyland P. L. (1986). Bifurcations of circle maps: Arnold tongues, bistability and rotation intervals. *Comm. Math. Phys.,* **106**(3), 353-381.

[5] Gardini L., V. Avrutin, I. Sushko. (2014). Codimension-2 border collision bifurcations in one-dimensional discontinuous piecewise smooth maps. *Int. J. Bif. Chaos*, **24** (2) 1450024 (30 pages).

[6] A.J. Homburg, Global aspects of homoclinic bifurcations of vector fields, Springer-Verlag, Berlin, 1996.

[7] S. Ito, S. Tanaka, and H. Nakada, On unimodal transformations and chaos II, Tokyo J. Math. 2 (1979), pp. 241–259.

[8] Keener J.P. (1980). Chaotic behavior in piecewise continuous difference equations. *Trans. Am. Math. Soc.,* **261**, 589–604.

[9] Leonov N.N. (1959). Map of the line onto itself. *Radiofisika,* **3**, 942–956.

[10] D.V. Lyubimov, A.S. Pikovsky, and M.A. Zaks, Universal scenarios of transitions to chaos via homoclinic bifurcations, Math. Phys. Rev. 8 (1989). Harwood Academic, London.

[11] Y.L. Maistrenko, V.L. Maistrenko, and L.O. Chua, Cycles of chaotic intervals in a time-delayed Chua's circuit, Int. J. Bifur. Chaos 3 (1993), pp. 1557–1572.

[12] K. Matsuyama. Custom versus Fashion: Path-dependence and Limit Cycles in a Random Matching Game. Discussion paper N 1030, 1992, Dept of Economics, Northwestern University.

[13] C. Mira. Embedding of a Dim1 Piecewise Continuous and Linear Leonov Map into a Dim2 Invertible Map. In: Global analysis of dynamic models for economics, finance and social sciences (G.-I. Bischi, C. Chiarella and I. Sushko Eds.), Springer, 2013.

[14] Nusse H.E , Yorke J.A. (1992). Border-collision bifurcations including period two to period three for piecewise smooth systems. Physica D, 57, 39–57.

[15] Nusse H.E., Yorke J.A. (1995). Border-collision bifurcations for piecewise smooth one-dimensional maps. *Int. J. Bif. Chaos,* **5**, 189–207.

[16] Panchuk A., Sushko I., Schenke B., Avrutin V. (2013). Bifurcation Structure in Bimodal Piecewise Linear Map. Int. J. Bif. Chaos, 23(12) 1330040 (24 pages).

[17] Simpson, D. J. W. & Meiss, J. D. (2008) Neimark-Sacker bifurcations in planar, piecewise-smooth, continuous maps, SIAM J. Appl. Dyn. Syst. 7, 795–824.

[18] I. Sushko, V. Avrutin, and L. Gardini, Bifurcation structure in the skew tent map and its application as a border collision normal form, J. Differ. Equ. Appl. (2015). doi:10.1080/10236198.2015.1113273

[19] I. Sushko, L. Gardini. Center Bifurcation for Two-Dimensional Border-Collision Normal Form, Int. J. Bifurcation and Chaos, Vol. 18, Issue 4 (2008), 1029-1050.

[20] Sushko I., L. Gardini, V. Avrutin. (2016). Nonsmooth One-dimensional Maps: Some Basic Concepts and Definitions. Journal of Difference Equations and Applications DOI: 10.1080/10236198.2016.1248426.

[21] F. Tramontana, I. Sushko, V. Avrutin. (2015). Period adding structure in a 2D discontinuous model of economic growth. Applied Mathematics and Computation, 253, 262273.

[22] Zh.T. Zhusubaliyev and E. Mosekilde, Bifurcations and Chaos in Piecewise-smooth Dynamical Systems, Nonlinear Science A Vol. 44, World Scientific, 2003.

[23] Z. T. Zhusubaliyev, E. Mosekilde, S. Maity, S. Mohanan, and S. Banerjee, Border collision route to quasi-periodicity: Numerical investigation and experimental confirmation, Chaos 16, 1054 (2006).